ISSN 1948-0210 (online)

World Journal of *Stem Cells*

World J Stem Cells 2024 April 26; 16(4): 324-461

Published by Baishideng Publishing Group Inc

World Journal of Stem Cells

Contents

Monthly Volume 16 Number 4 April 26, 2024

EDITORIAL

REVIEW

ORIGINAL ARTICLE

Basic Study

LETTER TO THE EDITOR

World Journal of Stem Cells

Monthly Volume 16 Number 4 April 26, 2024

Contents

ABOUT COVER

Editorial Board Member of *World Journal of Stem Cells*, Kun Xiong, PhD, Professor, Department of Anatomy and Neurobiology, School of Basic Medical Science, Central South University, Changsha 410013, Hunan Province, China. xiongkun2001@163.com

AIMS AND SCOPE

The primary aim of *World Journal of Stem Cells* (*WJSC*, *World J Stem Cells*) is to provide scholars and readers from various fields of stem cells with a platform to publish high-quality basic and clinical research articles and communicate their research findings online. *WJSC* publishes articles reporting research results obtained in the field of stem cell biology and regenerative medicine, related to the wide range of stem cells including embryonic stem cells, germline stem cells, tissue-specific stem cells, adult stem cells, mesenchymal stromal cells, induced pluripotent stem cells, embryonal carcinoma stem cells, hemangioblasts, lymphoid progenitor cells, *etc*.

INDEXING/ABSTRACTING

The *WJSC* is now abstracted and indexed in Science Citation Index Expanded (SCIE, also known as SciSearch®), Journal Citation Reports/Science Edition, PubMed, PubMed Central, Scopus, Biological Abstracts, BIOSIS Previews, Reference Citation Analysis, China Science and Technology Journal Database, and Superstar Journals Database. The 2023 Edition of Journal Citation Reports® cites the 2022 impact factor (IF) for *WJSC* as 4.1; IF without journal self cites: 3.9; 5-year IF: 4.5; Journal Citation Indicator: 0.53; Ranking: 15 among 29 journals in cell and tissue engineering; Quartile category: Q3; Ranking: 99 among 191 journals in cell biology; and Quartile category: Q3. The *WJSC*'s CiteScore for 2022 is 8.0 and Scopus CiteScore rank 2022: Histology is 9/57; Genetics is 68/325; Genetics (clinical) is 19/90; Molecular Biology is 119/380; Cell Biology is 95/274.

RESPONSIBLE EDITORS FOR THIS ISSUE

NAME OF JOURNAL
World Journal of Stem Cells

ISSN
ISSN 1948-0210 (online)

LAUNCH DATE
December 31, 2009

FREQUENCY
Monthly

EDITORS-IN-CHIEF
Shengwen Calvin Li, Carlo Ventura

EDITORIAL BOARD MEMBERS
https://www.wjgnet.com/1948-0210/editorialboard.htm

PUBLICATION DATE
April 26, 2024

INSTRUCTIONS TO AUTHORS
https://www.wjgnet.com/bpg/gerinfo/204

GUIDELINES FOR ETHICS DOCUMENTS
https://www.wjgnet.com/bpg/GerInfo/287

GUIDELINES FOR NON-NATIVE SPEAKERS OF ENGLISH
https://www.wjgnet.com/bpg/gerinfo/240

PUBLICATION ETHICS
https://www.wjgnet.com/bpg/GerInfo/288

PUBLICATION MISCONDUCT
https://www.wjgnet.com/bpg/gerinfo/208

ARTICLE PROCESSING CHARGE
https://www.wjgnet.com/bpg/gerinfo/242

STEPS FOR SUBMITTING MANUSCRIPTS
https://www.wjgnet.com/bpg/GerInfo/239

ONLINE SUBMISSION
https://www.f6publishing.com

World Journal of Stem Cells

Submit a Manuscript: https://www.f6publishing.com

World J Stem Cells 2024 April 26; 16(4): 389-409

DOI: 10.4252/wjsc.v16.i4.389

ISSN 1948-0210 (online)

ORIGINAL ARTICLE

Basic Study

Unveiling the role of hypoxia-inducible factor 2alpha in osteoporosis: Implications for bone health

Ling-Ling Wang, Zhan-Jin Lu, Shun-Kui Luo, Yun Li, Zhe Yang, Hong-Yun Lu

Specialty type: Cell and tissue engineering

Provenance and peer review: Unsolicited article; Externally peer reviewed.

Peer-review model: Single blind

Peer-review report's scientific quality classification

Grade A (Excellent): 0
Grade B (Very good): B, B, B
Grade C (Good): C, C
Grade D (Fair): 0
Grade E (Poor): 0

P-Reviewer: Ariga K, Japan; El-Akabawy G, Egypt; Roomi AB, Iraq; Ventura C, Italy

Received: November 9, 2023
Peer-review started: November 9, 2023
First decision: December 17, 2023
Revised: January 12, 2024
Accepted: February 21, 2024
Article in press: February 21, 2024
Published online: April 26, 2024

Ling-Ling Wang, Department of Gerontology, The Fifth Affiliated Hospital of Sun Yat-sen University, Zhuhai 519000, Guangdong Province, China

Zhan-Jin Lu, Shun-Kui Luo, Department of Endocrinology and Metabolism, The Fifth Affiliated Hospital of Sun Yat-sen University, Zhuhai 519000, Guangdong Province, China

Yun Li, Guangdong Provincial Key Laboratory of Biomedical Imaging, The Fifth Affiliated Hospital of Sun Yat-sen University, Zhuhai 519000, Guangdong Province, China

Zhe Yang, Hong-Yun Lu, Department of Endocrinology and Metabolism, Zhuhai People's Hospital (Zhuhai Clinical Medical College of Jinan University, the First Hospital Affiliated with Medical College of Macao University of Science and Technology), Zhuhai 519000, Guangdong Province, China

Corresponding author: Hong-Yun Lu, MD, PhD, Chief Doctor, Department of Endocrinology and Metabolism, Zhuhai People's Hospital (Zhuhai Clinical Medical College of Jinan University, the First Hospital Affiliated with Medical College of Macao University of Science and Technology), No. 79 Kangning Road, Zhuhai 519000, Guangdong Province, China.
luhongyun@jnu.edu.cn

Abstract

BACKGROUND

Osteoporosis (OP) has become a major public health problem worldwide. Most OP treatments are based on the inhibition of bone resorption, and it is necessary to identify additional treatments aimed at enhancing osteogenesis. In the bone marrow (BM) niche, bone mesenchymal stem cells (BMSCs) are exposed to a hypoxic environment. Recently, a few studies have demonstrated that hypoxia-inducible factor 2alpha (HIF-2α) is involved in BMSC osteogenic differentiation, but the molecular mechanism involved has not been determined.

AIM

To investigate the effect of HIF-2α on the osteogenic and adipogenic differentiation of BMSCs and the hematopoietic function of hematopoietic stem cells (HSCs) in the BM niche on the progression of OP.

METHODS

Mice with BMSC-specific HIF-2α knockout (Prx1-Cre;Hif-2α$^{fl/fl}$ mice) were used for *in vivo* experiments. Bone quantification was performed on mice of two genotypes

with three interventions: Bilateral ovariectomy, semilethal irradiation, and dexamethasone treatment. Moreover, the hematopoietic function of HSCs in the BM niche was compared between the two mouse genotypes. *In vitro*, the HIF-2α agonist roxadustat and the HIF-2α inhibitor PT2399 were used to investigate the function of HIF-2α in BMSC osteogenic and adipogenic differentiation. Finally, we investigated the effect of HIF-2α on BMSCs *via* treatment with the mechanistic target of rapamycin (mTOR) agonist MHY1485 and the mTOR inhibitor rapamycin.

RESULTS

The quantitative index determined by microcomputed tomography indicated that the femoral bone density of Prx1-Cre;Hif-2α$^{fl/fl}$ mice was lower than that of Hif-2α$^{fl/fl}$ mice under the three intervention conditions. *In vitro*, Hif-2α$^{fl/fl}$ mouse BMSCs were cultured and treated with the HIF-2α agonist roxadustat, and after 7 d of BMSC adipogenic differentiation, the oil red O staining intensity and mRNA expression levels of adipogenesis-related genes in BMSCs treated with roxadustat were decreased; in addition, after 14 d of osteogenic differentiation, BMSCs treated with roxadustat exhibited increased expression of osteogenesis-related genes. The opposite effects were shown for mouse BMSCs treated with the HIF-2α inhibitor PT2399. The mTOR inhibitor rapamycin was used to confirm that HIF-2α regulated BMSC osteogenic and adipogenic differentiation by inhibiting the mTOR pathway. Consequently, there was no significant difference in the hematopoietic function of HSCs between Prx1-Cre;Hif-2α$^{fl/fl}$ and Hif-2α$^{fl/fl}$ mice.

CONCLUSION

Our study showed that inhibition of HIF-2α decreases bone mass by inhibiting the osteogenic differentiation and increasing the adipogenic differentiation of BMSCs through inhibition of mTOR signaling in the BM niche.

Key Words: Hypoxia-inducible factor-2α; Bone marrow niche; Bone mesenchymal stem cells; Osteoporosis; Osteogenic/adipogenic differentiation; Mechanistic target of rapamycin signaling pathway

Core Tip: This manuscript explores the role of hypoxia-inducible factor 2alpha (HIF-2α) in bone mesenchymal stem cell (BMSC) osteogenic differentiation in the bone marrow niche, a role that is still unclear and controversial, *via in vivo* and *in vitro* experiments. We verified that downregulation of HIF-2α inhibits osteogenesis *in vivo* by generating mice with BMSC-specific HIF-2α knockout and applying interventions such as bilateral ovariectomy, semilethal irradiation, and treatment with dexamethasone. *In vitro*, we found that downregulation of HIF-2α can inhibit osteogenesis and increase adipogenesis by suppressing the mechanistic target of rapamycin signaling pathway, which may lead to the identification of drug target genes for the clinical treatment of osteoporosis.

Citation: Wang LL, Lu ZJ, Luo SK, Li Y, Yang Z, Lu HY. Unveiling the role of hypoxia-inducible factor 2alpha in osteoporosis: Implications for bone health. *World J Stem Cells* 2024; 16(4): 389-409
URL: https://www.wjgnet.com/1948-0210/full/v16/i4/389.htm
DOI: https://dx.doi.org/10.4252/wjsc.v16.i4.389

INTRODUCTION

Osteoporosis (OP) is a disorder associated with a decrease in bone mineral density (BMD), a low bone mass and increased bone fragility, and it increases the risk of fragility fractures. The economic and social burden of fragility fractures is massive, previously estimated at 37 billion euros per year in 27 European countries alone[1]. OP has become an important public health problem in China. From December 2017 to August 2018, the China Osteoporosis Prevalence Study enrolled a representative sample of 20416 participants aged 20 years or older from mainland China, and the overall prevalence of OP was 20.6% among women aged 40 years or older and 5.0% among men aged 40 years or older. The prevalence of OP among postmenopausal women was 32.1%, and the prevalence of OP among men aged 50 years or older was 6.9%. The prevalence of vertebral fracture was 10.5% among men and 9.7% among women[2]. Therefore, it is important for us to investigate the mechanism of OP.

Bone is a highly dynamic tissue with continuous remodeling at the surface that supports body weight and maintains mineral homeostasis. Bone homeostasis requires coordinated activities between osteoblasts and osteoclasts. Osteoblasts are responsible for the deposition of bone matrix on the bone surface, and osteoclasts are responsible for bone resorption [3]. Age-related (type II) OP is a common and debilitating condition driven in part by the loss of bone marrow (BM) mesenchymal stromal cells and their osteoblast progeny, leading to reduced bone formation. Current pharmacological regimens targeting age-related OP do not directly treat the disease by increasing bone formation but instead use bisphosphonates to reduce bone resorption - a treatment approach designed for postmenopausal (type-I) OP[4]. It is important to identify an OP treatment focused on increasing bone formation.

Bone mesenchymal stem cells (BMSCs) are multipotent marrow stromal cells. Upon exposure to different extracellular stimuli, different sets of signaling pathways and transcription factors are activated or inhibited in BMSCs, leading to distinct fates of differentiation into cells of different lineages, such as osteoblasts (bone-forming cells), chondrocytes (cartilage cells) and marrow adipocytes (fat cells). The two other major functions of BMSCs include functioning as cellular components of the hematopoietic stem cell (HSC) niche and immunosuppression[5]. In the BM, BMSCs are exposed to a hypoxic environment. Spencer *et al*[6] performed direct *in vivo* measurements of local oxygen tension (pO_2) in the BM of live mice. Using two-photon phosphorescence lifetime microscopy, the authors determined that the absolute pO2 of the BM was quite low (< 32 mmHg). Cellular adaptation to hypoxia is mediated in part by hypoxia-inducible factors (HIFs). HIFs are composed of two subunits, an O_2-labile α subunit (HIF-1α, HIF-2α, or HIF-3α) and a constitutively expressed β subunit (HIF-1β, also known as aryl hydrocarbon receptor nuclear translocator)[7]. Tissue-specific deletion of HIF1α, HIF 2α, or the HIF-α degradation machinery component proline hydroxylase domain 2 (Phd2) or von Hippel-Lindau (Vhl) results in a variety of skeletal phenotypes that underscore the complexity of skeletal HIF-α signaling during development and disease[8]. Briefly, hypoxia and HIF-α promote skeletal mesenchymal condensation and limb development, promoting chondrogenesis by increasing Sox9 expression and reducing osteogenesis through Runx2 inhibition[9]. Most of the results showed that HIF-1α represents a potential therapeutic target for preventing osteoclast activation and bone loss in postmenopausal patients[10]. Recently, a few studies have demonstrated that HIF-2α is involved in BMSC osteogenic differentiation, but the molecular mechanism and role of HIF-2α in hematopoietic function in the BM niche have not been determined.

In this study, we generated mice with BMSC-specific HIF-2α knockout (Prx1-Cre;Hif-2α$^{fl/fl}$ mice) to study the osteogenic/adipogenic differentiation capacity of BMSCs and the hematopoietic microenvironment of HSCs in order to reveal the influence of HIF-2α regulation in the BM niche on OP, determine the related mechanism, and identify drug target genes that promote bone formation for the clinical treatment of OP.

MATERIALS AND METHODS

Mice

Hif-2α$^{fl/fl}$ mice (008407-Epas1tm1Mcs/J) were purchased from the Jackson Laboratory. Hif-2α$^{fl/fl}$ mice were crossed with Prx-1-Cre transgenic mice (kindly provided by Professor Meng Zhao (Sun Yat-sen University, Guangzhou, China) to produce mice with conditional knockout of HIF-2α in BMSCs (Prx-1-Cre;Hif-2α$^{fl/fl}$ mice). Age- and sex-matched WT littermates (Hif-2α$^{fl/fl}$) were used as controls. The primers used for genotyping are listed in Table 1. Hif-2α$^{fl/fl}$ and Prx-1-Cre;Hif-2α$^{fl/fl}$ mice were subjected to ovariectomy, dexamethasone (DEX) treatment, or semilethal irradiation. Mice of the same age (6-8 wk), sex, and genotype were randomly grouped for subsequent experiments (the investigators were not blinded). No sex-related differences were observed in the Prx-1-Cre;Hif-2α$^{fl/fl}$ mice. All animals were maintained under specific pathogen-free conditions and fed a standard diet.

Microcomputed tomography

The harvested bones were fixed for 48 h in 4% paraformaldehyde and then dehydrated in 80% ethanol. By using a microcomputed tomography (μCT) 100 scanner (isotropic voxel size of 10 μm, 70 kVp, 200 μA, integration time of 200 ms; Scanco Medical, Switzerland), femora were analyzed as previously described[11]. Determination of the trabecular and cortical bone volume (BV) fractions [BV/total volume (TV)], BMD, thickness (trabecular thickness), trabecular number and trabecular separation was performed using established analysis protocols, and the μCT parameters were reported according to international guidelines.

Ovariectomy-induced OP

For OP induction by ovariectomy, 8-wk-old virgin female mice were anesthetized with 10 μL/g 0.6% pentobarbital sodium, the fur was shaved, and the skin was disinfected with betadine. A dorsal midline incision was made, and the periovarian fat pad was gently grasped to exteriorize the ovary. The fallopian tube was then clamped, and the ovary was removed by cutting above the clamped site. The uterine horn was returned to the abdomen, and the same process was repeated on the other side. After surgery, antibiotic water (250 mL sterile water + 2.5 mL of enrofloxacin) was provided for one week, and the mice were closely monitored until they resumed full activity[12].

DEX treatment

Two-month-old Prx1-Cre;Hif-2α$^{fl/fl}$ and Hif-2α$^{fl/fl}$ male mice were treated with daily intraperitoneal injection of phosphate buffered saline or 20 mg/kg DEX for 28 d[12].

Semilethal irradiation

Both Prx1-Cre;Hif-2α$^{fl/fl}$ and Hif-2α$^{fl/fl}$ male mice received whole-body X-irradiation (4.5 Gy, semilethal dose; Rs2000, Rad Source). After surgery, the mice were provided antibiotic water (250 mL sterile water + 2.5 mL enrofloxacin) for 1 wk[13]. Peripheral blood (PB) was collected from individual mice in heparin-coated capillary tubes to measure white blood cell (WBC) counts on days 0, 7, 14, 21, 28, and 42 after semilethal irradiation.

5-fluorouracil treatment

5-fluorouracil (5-FU) was administered intraperitoneally to Prx1-Cre;Hif-2α$^{fl/fl}$ andHif-2α$^{fl/fl}$ mice once a week for 2 wk at a

Table 1 Genotyping primers

Primers	Sequence	Amplicon
HIF2α	F: 5′-GAGAGCAGCTTCTCCTGGAA-3′	WT182 bp
	R: 5′-TGTAGGCAAGGAAACCAAGG-3′	MT220 bp
Prx-1	F: 5′-GCGGTCTGGCAGTAAAAACTATC-3′	100 bp
	R: 5′-GTGAAACAGCATTGCTGTCACTT-3′	

dose of 150 mg/kg body weight[14].

Blood cell counts

PB was collected from the tail vein and analyzed using a ProCyte Dx Hematology Analyzer (IDEXX).

BM digestion

Enzymatic digestion of BM was performed as described previously[15]. Briefly, intact marrow plugs were flushed from the long bones and subjected to two rounds of enzymatic digestion at 37 °C for 20 min each. The digestion buffer contained 3 mg/mL type I collagenase, 4 mg/mL dispase, and 1 U/mL DNase I in HBSS supplemented with calcium and magnesium. The cells were resuspended in staining medium (HBSS + 2% fetal bovine serum) to terminate digestion.

Fibroblast colony-forming unit assay

BM cells were collected from the bilateral femora of the mice and subjected to fibroblast colony-forming unit (CFU-F) assays as previously described[16]. Briefly, 10^6 cells were cultured for 7 d. The cells were stained with 0.1% crystal violet, and colony-forming units were counted under a microscope[13].

Fluorescence-activated cell sorting analysis

BMSCs were identified by the expression of PDGFRα[17] and CD51[18]. For classification of HSCs, long-term HSCs were defined as $Lin^-Sca1^+c\text{-}KIT^+$ (LSK) $CD34^-FLK2^-$ cells; short-term HSCs, as $LSKCD34^+FLK2$ $cells^-$; multipotent progenitors, as $LSKCD150^-CD48^-$ cells; and HSCs, as $LSKCD150^+CD48^-$ cells. For classification of hematopoietic progenitor cells (HPCs), common myeloid progenitors were defined as $Lin^-c\text{-}Kit^+Sca\text{-}1^-CD16/32^{med}CD34^+$ cells; common lymphoid progenitors, as $Lin^-c\text{-}Kit^{low}Sca\text{-}1^{low}CD127^+$ cells; and granulocyte-monocyte progenitors, as $Lin^-c\text{-}Kit^+Sca\text{-}1^-CD16/32^{high}CD34^+$ cells; and megakaryocyte-erythroid progenitors, as $Lin^-c\text{-}Kit^+Sca\text{-}1^-CD16/32^{med/Low}CD34^-$ cells.

For cell cycle analysis, BM cells freshly harvested from femora and tibiae were stained with antibodies conjugated to various fluorochromes, fixed and permeabilized with 0.2% Triton X-100, stained with an Alexa Fluor 488-conjugated anti-Ki-67 antibody, and further incubated with DAPI (0.1 mg/mL)[14].

In vitro differentiation

Equal numbers of cultured cells from Hif-$2\alpha^{fl/fl}$ and Prx1-Cre;Hif-$2\alpha^{fl/fl}$ mice were replated to ensure that there was no difference in the density of the cells of the different genotypes. On the second day of culture, the medium was replaced with adipogenic (7 d) or osteogenic (7 d or 14 d) differentiation medium. The osteogenic differentiation medium consisted of MEM supplemented with 10 mmol/L β-glycerol phosphate disodium salt, 10 nM DEX (D1756) and 50 μM L-ascorbic acid[19]. Fourteen days later, the percentage of colonies that contained osteoblasts was quantified by alizarin red staining (1%, pH = 4.2; Solarbio). Adipogenic differentiation was induced by the addition of α-MEM containing 10% fetal calf serum, insulin (1 μg/mL; Sigma), 1 μM DEX (Sigma), and 0.5 mmol/L 3-isobutyl-1-methylxanthine (Sigma). The differentiation of adipocytes was monitored by Oil red O staining[11].

Quantitative real-time polymerase chain reaction

Total RNA was extracted from cells and tissues according to the Trizol reagent RNA extraction protocol (Magen). cDNA was obtained by reverse transcription of 1 μg of RNA according to the manufacturer's instructions (Takara). Gene expression levels were measured using real-time polymerase chain reaction (RT-PCR) with a CFX96 Touch. The primers used are listed in Table 2. Actin was used as an internal control.

Western blot analysis

Total protein was extracted from cells and tissues with radioimmunoprecipitation assay buffer. Equal amounts of extracted proteins were separated *via* 12.5% sodium-dodecyl sulfate gel electrophoresis and transferred to a polyvinylidene fluoride membrane. After blocking with 5% nonfat milk in Tris-buffered saline with Tween 20 (TBST, pH = 7.6) for 1 h at room temperature, the membranes were incubated with primary antibodies [specific for mechanistic target of rapamycin (mTOR), AKT, and β-actin] overnight at 4 °C and then incubated with secondary antibodies (rabbit, 1:10000) for 1 h at room temperature. Western blot images were acquired with a ChemiDoc XRS imaging system (Bio-Rad).

Table 2 Primers used for quantitative real-time polymerase chain reaction of total RNA

Genes	Primers types	Sequence (5'-3')
HIF-2α	Forward	CTCCCACCTGGACAAAGC
	Reverse	GTCGCAAGGATGAGTGAAGT
HIF-2α exon2	Forward	ACAAAGCCTCCATCATGCG
	Reverse	CGTCTTGGGTCACCACAG
Runx2	Forward	TCCACAAGGACAGAGTCAGATTACAG
	Reverse	CAGAAGTCAGAGGTGGCAGTGTCATC
Col1α1	Forward	TGTGTGCGATGACGTGCAAT
	Reverse	GGGTCCCTCGACTCCTACA
OCN	Forward	AGACTCCGGCGCTACCTT
	Reverse	AAGCAGGGTCAAGCTCACAT
CEBPa	Forward	CAAGAACAGCAACGAGTACCG
	Reverse	GTCACTGGTCAACTCCAGCAC
Lpl	Forward	GCGTAGCAGGAAGTCTGACCAA
	Reverse	AGCGTCATCAGGAGAAAGGCGA
Adipo-nectin	Forward	TGTTCCTCTTAATCCTGCCCA
	Reverse	CCAACCTGCACAAGTTCCCTT
PI3K	Forward	ACACCACGGTTTGGACTATGG
	Reverse	GGCTACAGTAGTGGGCTTGG
AKT	Forward	TGGGTCAAGGAACAGAAGCA
	Reverse	TCACACTGACCACTGACACA
mTOR	Forward	CGGGACTCTTTACACTGCG
	Reverse	CCTTCAGGCTCAACCAACA
Actin	Forward	TTGCTGACAGGATGCAGAAGGAGA
	Reverse	ACTCCTGCTTGCTGATCCACATCT

HIF-2α: Hypoxia-inducible factor 2alpha; mTOR: Mechanistic target of rapamycin.

Statistical analysis

All the statistical analyses were performed with GraphPad Prism (version 8.0). The statistical significance of differences between two groups was determined using unpaired Student's *t* test (two-sided), unless otherwise specified in the figure legends. In all the studies, the data are shown as the mean ± SD values, and statistically significant differences are indicated in the figures; $^{a}P < 0.05$, $^{b}P < 0.01$, $^{c}P < 0.001$.

RESULTS

Generation of a mouse model with BMSC-specific knockout of HIF-2α

To assess the physiological function of HIF-2α in early osteoblast lineage cells, we generated HIF-2α CKO mice with Prx-1-Cre transgenic mice (Figure 1A), which express Cre recombinase in BMSCs. Briefly, we mated floxed HIF-2α mice with Prx1-Cre transgenic mice to generate Prx1-Cre;Hif-2α$^{wt/fl}$ mice, which were mated with Hif-2α$^{fl/fl}$ mice to generate Hif-2α$^{fl/fl}$ mice, Prx1-Cre;Hif-2α$^{wt/fl}$ mice, and Prx1-Cre;Hif-2α$^{fl/fl}$ mice. Littermate mice were used in all the experiments. The genotyping primers used are listed in Table 1, and the DNA genotyping results are shown in Figure 1B and C. Mice with the above genotypes were born at normal Mendelian ratios and did not exhibit significant weight or developmental differences (Figure 2A and B). To confirm the deletion of HIF-2α in Prx1-Cre;Hif-2α$^{fl/fl}$ BMSCs, the HIF-2α protein expression was analyzed in BMSCs, and HIF-2α was found to be efficiently deleted in most BMSCs from Prx1-Cre;Hif-2α$^{fl/fl}$ mice (Figure 1D). Moreover, quantitative RT-PCR analysis of total RNA extracted from BMSCs and from the spleen, muscle, and liver showed that the expression levels of HIF-2α mRNA (Figure 1E) and HIF-2α exon 2 (Figure 1I) were significantly lower in the BMSCs of Prx1-Cre;Hif-2α$^{fl/fl}$ mice than in those of Hif-2α$^{fl/fl}$ mice, but there were no differences

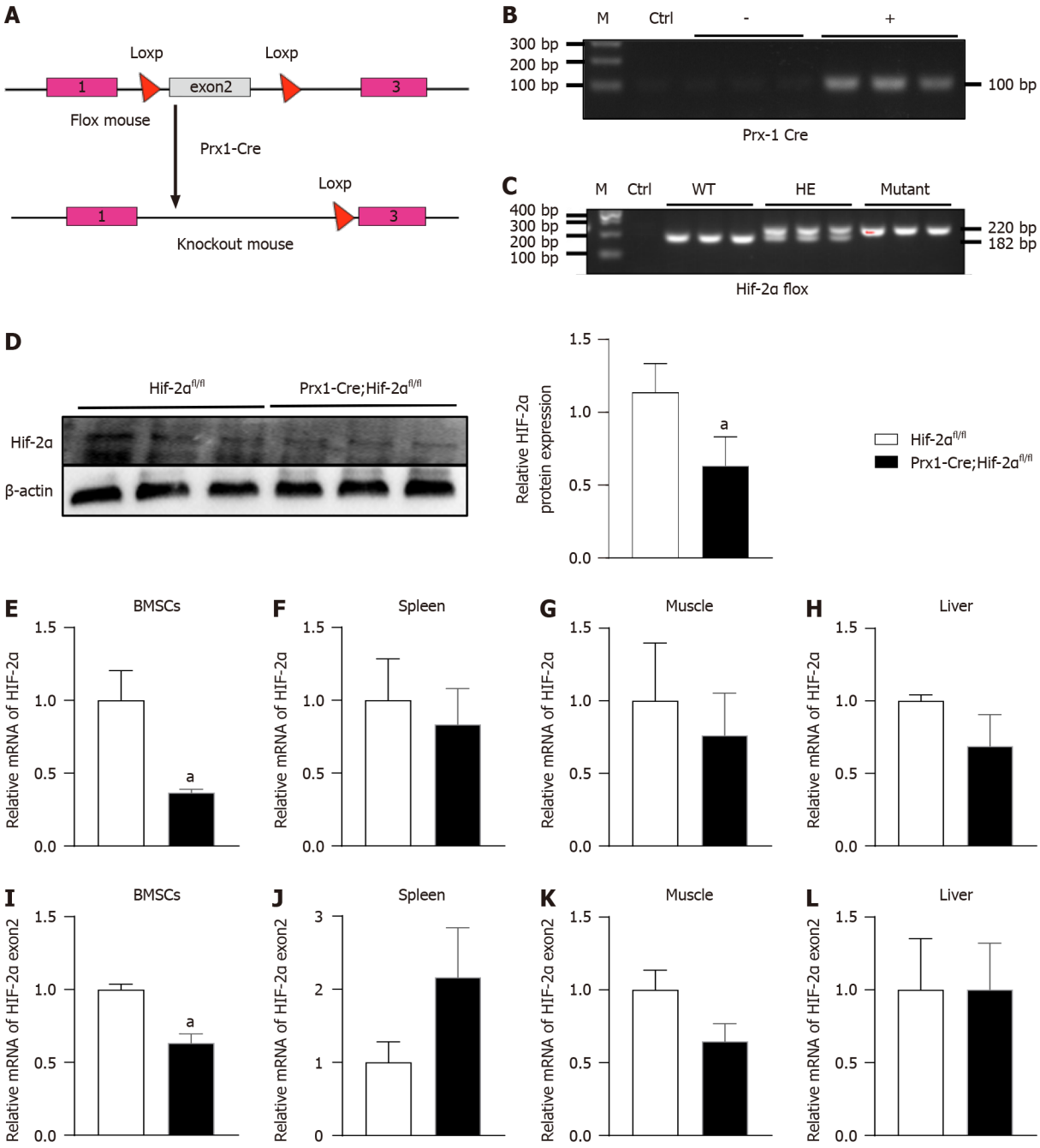

Figure 1 Generation of mice with bone mesenchymal stem cell-specific hypoxia-inducible factor 2alpha-KO. A: The mouse mating process; B: Prx-1 Cre gene identification; 100 bp is the positive band; C: Hypoxia-inducible factor 2alpha (HIF-2α) gene identification; 220 bp is the target band, 182 bp is the WT band; D: The differences in protein expression in primary bone mesenchymal stem cells (BMSCs) isolated from Prx1-Cre;Hif-2α$^{fl/fl}$ and Hif-2α$^{fl/fl}$ mice; E-L: HIF-2α (E) and HIF-2α Exon2 (I) transcript levels in BMSCs in Prx1-Cre;Hif-2α$^{fl/fl}$ and Hif-2α$^{fl/fl}$ mice; HIF-2α (F) and HIF-2α Exon2 (J) transcript levels in spleens of Prx1-Cre;Hif-2α$^{fl/fl}$ and Hif-2α$^{fl/fl}$ mice; HIF-2α (G) and HIF-2α Exon2 (K) transcript levels in muscles of Prx1-Cre;Hif-2α$^{fl/fl}$ and Hif-2α$^{fl/fl}$ mice; HIF-2α (H) and HIF-2α Exon2 (L) transcript levels in livers of Prx1-Cre;Hif-2α$^{fl/fl}$ and Hif-2α$^{fl/fl}$ mice; $^{a}P < 0.05$. BMSC: Bone mesenchymal stem cell; HIF-2α: Hypoxia-inducible factor 2alpha.

in these levels in the spleen (Figure 1F and J), muscle (Figure 1G and K) or liver (Figure 1H and L) between the two genotypes of mice. Next, we used μCT and hematoxylin and eosin staining to evaluate the effects of HIF-2α deletion on bone morphometry. μCT analysis revealed that there were no differences in bone mass between Prx1-Cre;Hif-2α$^{fl/fl}$ and Hif-2α$^{fl/fl}$ mice (Figure 3A and C-F). Hematoxylin and eosin staining[20] also showed that there were no differences in bone mass between Prx1-Cre;Hif-2α$^{fl/fl}$ and Hif-2α$^{fl/fl}$ mice (Figure 3B and G-I). Furthermore, as BMSCs are the major source cells for bone formation, we determined the number of BMSCs in Prx1-Cre;Hif-2α$^{fl/fl}$ and Hif-2α$^{fl/fl}$ mice. Fluorescence-activated cell sorting (FACS) analysis showed that the frequency of BMSCs was significantly reduced in Prx1-Cre;Hif-2α$^{fl/fl}$ mice (Figure 3J and K).

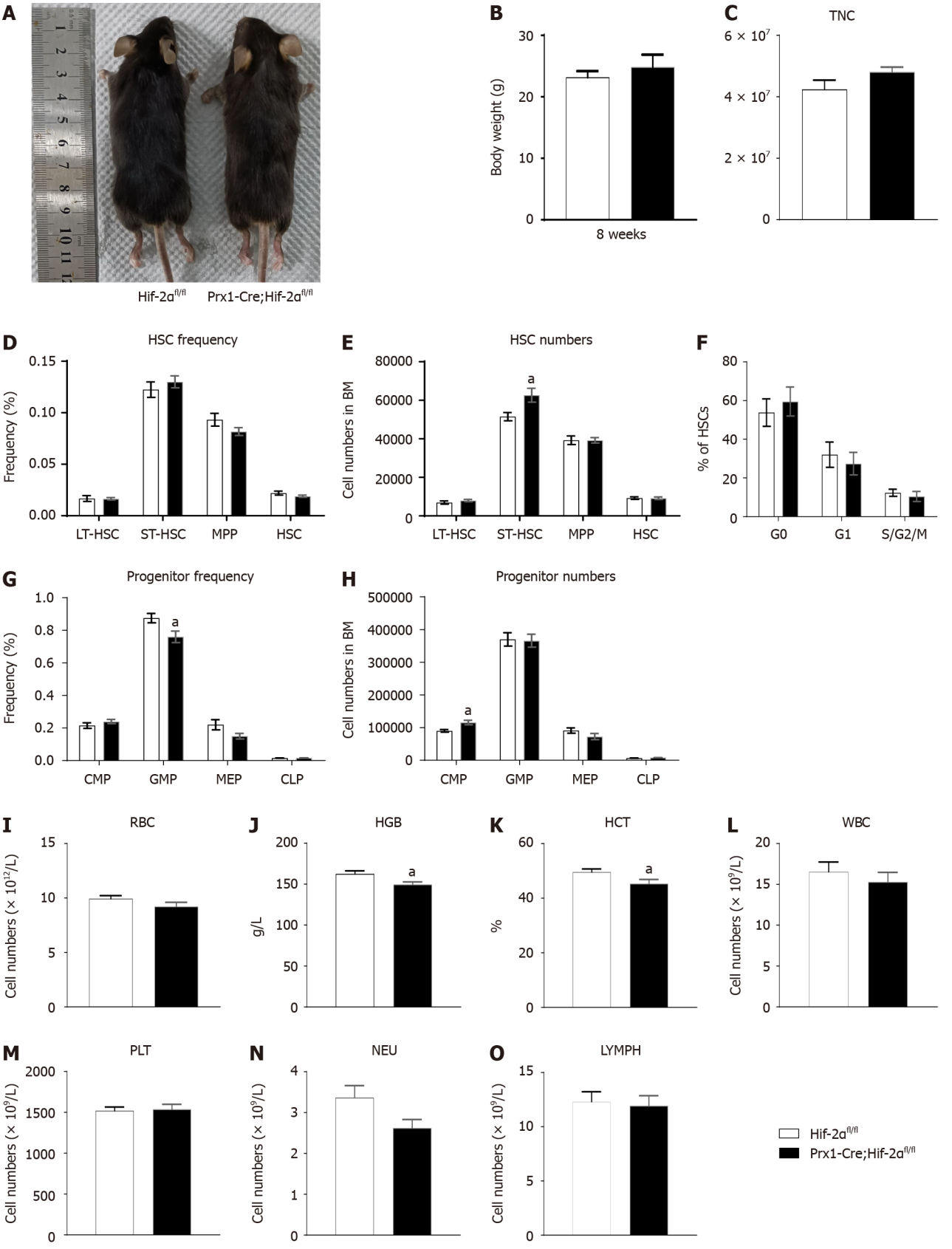

Figure 2 Hypoxia-inducible factor 2alpha-deficient mice were grossly developmentally normal and exhibited mild anemia but normal hematopoiesis. A: Representative images of two-month-old Prx1-Cre;Hif-2α$^{fl/fl}$ and Hif-2α$^{fl/fl}$ mice; B: Body masses of 2-month-old Prx1-Cre;Hif-2α$^{fl/fl}$ and Hif-2α$^{fl/fl}$ mice; C: Total nucleated cells in bone marrow (BM); D-O: BM cells freshly harvested from 8-wk-old Prx1-Cre;Hif-2α$^{fl/fl}$ and Hif-2α$^{fl/fl}$ mice were assayed by multiparametric fluorescence-activated cell sorting (FACS) analyses to determine the frequencies of hematopoietic stem cells (HSCs) (D), HSC numbers (E), frequencies of progenitors (G), and progenitor numbers (H); BM cells harvested from Prx1-Cre;Hif-2α$^{fl/fl}$ and Hif-2α$^{fl/fl}$ mice were assayed by FACS to determine the cell cycle status of HSCs. The percentages of HSCs in G0, G1, and S/G2/M phases (F) were quantified; erythrocyte count (I), hemoglobin content (J), hematocrit

value (K), white blood cell count (L), platelet count (M), neutrophil count (N), and lymphocyte count (O) in peripheral blood of Prx1-Cre;Hif-2α$^{fl/fl}$ and Hif-2α$^{fl/fl}$ mice; $^{a}P < 0.05$. TNC: Total nucleated cell; HSC: Hematopoietic stem cell; LT-HSC: Long-term hematopoietic stem cell; ST-HSC: Short-term hematopoietic stem cell; MPP: Multipotent progenitor; MSC: Mesenchymal stem cell; CMP: Common myeloid progenitor; GMP: Granulocyte-monocyte progenitor; MEP: Megakaryocyte-erythroid progenitor; CLP: Common lymphoid progenitor; RBC: Red blood cell; HGB: Hemoglobin; HCT: Hematocrit; WBC: White blood cell; PLT: Platelet; NEU: Neutrophil; LYMPH: Lymphocyte; HIF-2α: Hypoxia-inducible factor 2alpha.

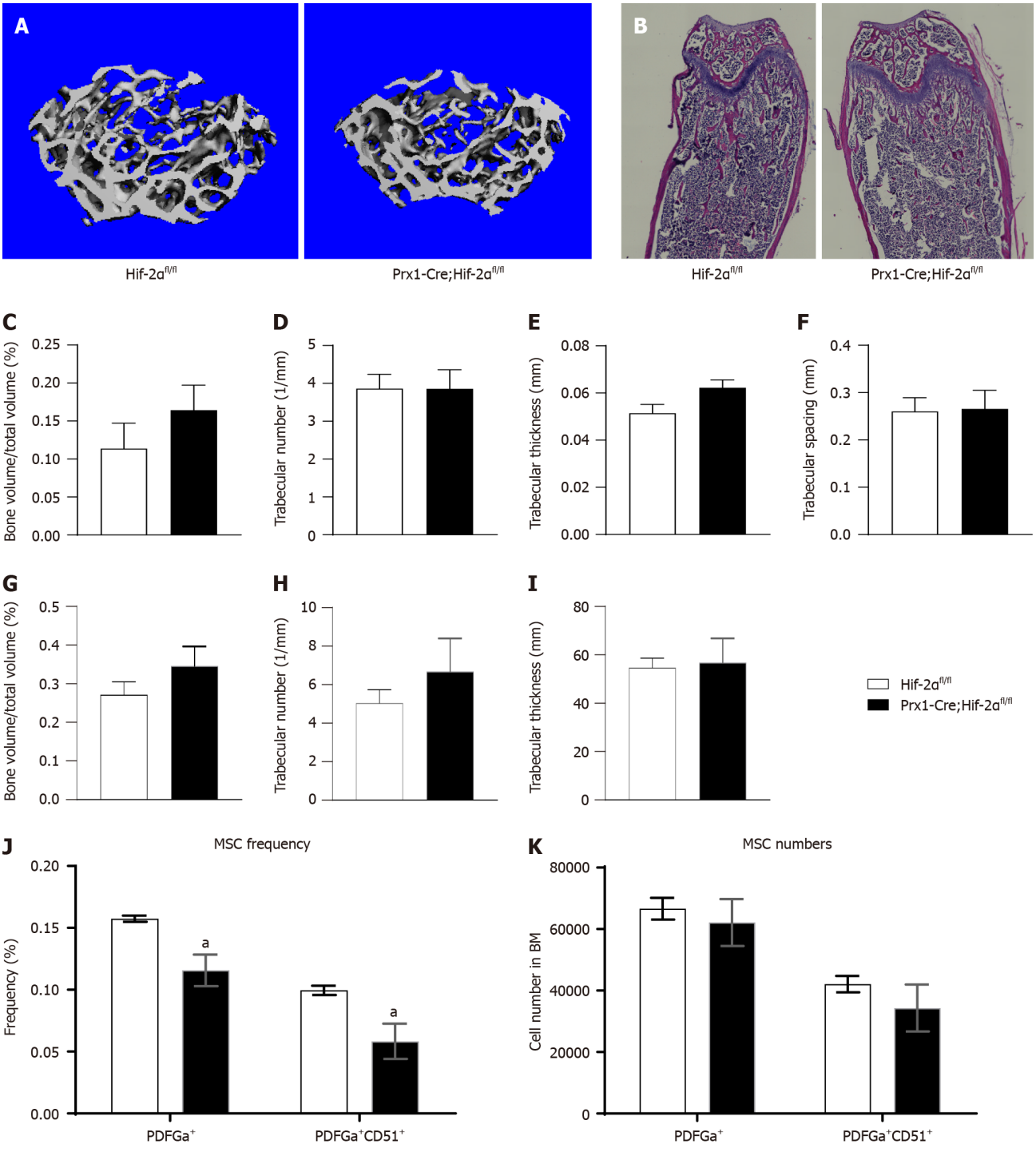

Figure 3 Adult Prx1-Cre;Hif-2α$^{fl/fl}$ and Hif-2α$^{fl/fl}$ mice exhibit no difference in bone mass under the naive condition. A: Microcomputed tomography (μCT) reconstruction images of distal femoral metaphyses from 2-month-old Prx1-Cre;Hif-2α$^{fl/fl}$ and Hif-2α$^{fl/fl}$ mice; B: Hematoxylin and eosin (HE) staining images of distal femoral metaphyses from 2-month-old Prx1-Cre;Hif-2α$^{fl/fl}$ and Hif-2α$^{fl/fl}$ mice; C-K: Quantitative μCT analyses of the structural parameters of femoral trabeculae from 2-month-old mice: bone volume/tissue volume (C), trabecular number (D), trabecular thickness (E), and trabecular spacing (F); quantitative HE staining analysis of the structural parameters of femoral trabeculae from 2-month-old mice: bone volume/tissue volume (G), trabecular number (H), and trabecular thickness (I); bone marrow cells freshly harvested from 8-wk-old Prx1-Cre;Hif-2α$^{fl/fl}$ and Hif-2α$^{fl/fl}$ mice were assayed by multiparameter fluorescence-activated cell sorting analyses to

determine the frequency (J) and number (K) of bone mesenchymal stem cells. [a]*P* < 0.05. MSC: Mesenchymal stem cell.

Mice with BMSC-specific HIF-2α knockout exhibited significantly reduced femoral bone density, which exacerbated the occurrence and development of OP in these mice

As there was a difference in the frequency of BMSCs between Prx1-Cre;Hif-2α$^{fl/fl}$ and Hif-2α$^{fl/fl}$ mice, we used 3 different interventions to modulate the bone mass in these mice. μCT analysis revealed an osteopenic phenotype in Prx1-Cre;Hif-2α$^{fl/fl}$ mice after each of the 3 interventions.

First, 4 wk after bilateral ovariectomy, clinical postmenopausal OP was simulated in female mice. Differences in bone phenotypes between the two genotypes of mice were quantified by μCT. Figure 4A shows the three-dimensional μCT reconstructions of the distal femora of mice of the different genotypes. Quantitative analysis indicated that, compared with those in Hif-2α$^{fl/fl}$ mice, the trabecular BV (Figure 4B) and trabecular thickness (Figure 4D) was decreased, the trabecular number (Figure 4C) and the bone mineral density (Figure 4E) was decreased, and the trabecular separation (Figure 4F) was increased in Prx1-Cre;Hif-2α$^{fl/fl}$ mice. The above results suggest that after bilateral ovariectomy, the bone mass of Prx1-Cre;Hif-2α$^{fl/fl}$ mice decreased significantly compared with that of Hif-2α$^{fl/fl}$ mice.

Second, semilethal irradiation was used to induce OP in mice of different genotypes. Differences in bone phenotypes between mice of the two genotypes were quantified by μCT. Figure 4G shows the three-dimensional μCT reconstructions of the distal femora of mice of the different genotypes. Analysis of the quantitative indicators suggested that the trabecular BV (BV/TV, as shown in Figure 4H) and trabecular number (Figure 4I) were decreased and the trabecular separation (Figure 4L) was increased in Prx1-Cre;Hif-2α$^{fl/fl}$ mice compared with Hif-2α$^{fl/fl}$ mice and that the trabecular thickness (Figure 4J) and the bone mineral density (Figure 4K) was decreased in Prx1-Cre;Hif-2α$^{fl/fl}$ mice compared to WT mice. Taken together, these results suggest that after semilethal irradiation, the bone mass of Prx1-Cre;Hif-2α$^{fl/fl}$ mice decreased significantly compared with that of Hif-2α$^{fl/fl}$ mice.

Mice of the different genotypes were treated with DEX, and after 4 wk, the differences in bone phenotypes between the two genotypes were quantified *via* μCT. Figure 4M shows the three-dimensional μCT reconstructions of the distal femora of mice of the different genotypes, and analysis of the quantitative indicators indicated a decrease in the trabecular number (Figure 4O) and an increase in the trabecular separation (Figure 4R) in Prx1-Cre;Hif-2α$^{fl/fl}$ mice compared with Hif-2α$^{fl/fl}$ mice. Similarly, compared with that in Hif-2α$^{fl/fl}$ mice, the trabecular BV (BV/TV, as shown in Figure 4N) in Prx1-Cre;Hif-2α$^{fl/fl}$ mice was decreased. There were no differences in the trabecular thickness (Figure 4P) or BMD (Figure 4Q) between the two genotypes of mice. The above results suggested that, after DEX treatment, the bone mass of Prx1-Cre;Hif-2α$^{fl/fl}$ mice decreased significantly compared to that of WT mice.

BMSC-specific knockout of HIF-2α had no significant effect on the hematopoietic function of HSCs or HPCs

As the above results revealed the difference in bone mass between Prx1-Cre;Hif-2α$^{fl/fl}$ and Hif-2α$^{fl/fl}$ mice, the effect of HIF-2α in the BM microenvironment on the hematopoietic functions of HSCs and HPCs was deemed worthy of investigation. Under naive conditions, tail vein blood of Prx1-Cre;Hif-2α$^{fl/fl}$ and Hif-2α$^{fl/fl}$ mice was analyzed *via* a PB test. The results indicated that the concentration of hemoglobin (HGB, as shown in Figure 2J) in Prx1-Cre;Hif-2α$^{fl/fl}$ mice was 149 g/L, the HGB concentration in Hif-2α$^{fl/fl}$ mice was 163 g/L, the hematocrit (HCT, as shown in Figure 2K) in Prx1-Cre;Hif-2α$^{fl/fl}$ mice was 45%, and the HCT in Hif-2α$^{fl/fl}$ mice was 49.6%, but no significant differences were observed in the RBC (Figure 2I), leukocyte (WBC, as shown in Figure 2L), neutrophil/granulocyte (NEU, as shown in Figure 2N), lymphocyte (LYMPH, as shown in Figure 2O) and platelet (PLT, as shown in Figure 2M) counts between the two genotypes of mice.

Furthermore, we isolated the total nucleated cell (TNC) population from the BM of Prx1-Cre;Hif-2α$^{fl/fl}$ and Hif-2α$^{fl/fl}$ mice for analysis. First, we analyzed the TNC number (as shown in Figure 2C) and found no significant difference between the two genotypes. Then, we analyzed the total number (Figure 2E) and proportion (Figure 2D) of HSCs in Prx1-Cre;Hif-2α$^{fl/fl}$ mice and Hif-2α$^{fl/fl}$ mice and found that there were no significant differences. Furthermore, we analyzed the cell cycle distribution of HSCs from Prx1-Cre;Hif-2α$^{fl/fl}$ mice and from Hif-2α$^{fl/fl}$ mice and found no significant differences (Figure 2F). Moreover, we analyzed the total number (Figure 2H) and proportion (Figure 2G) of HPCs in Prx1-Cre;Hif-2α$^{fl/fl}$ mice and Hif-2α$^{fl/fl}$ mice, and the results did not reveal significant differences. In general, the BMSC population in Prx1-Cre;Hif-2α$^{fl/fl}$ mice was significantly reduced under naive conditions, but there were no significant differences in the BM HSC and HPC populations in Prx1-Cre;Hif-2α$^{fl/fl}$ mice compared with Hif-2α$^{fl/fl}$ mice; thus, genetic deletion of HIF-2α in BMSCs had no effect on the hematopoietic microenvironment.

Under naive conditions, there were no significant differences in the hematopoietic phenotype between Prx1-Cre;Hif-2α$^{fl/fl}$ mice and Hif-2α$^{fl/fl}$ mice. To further clarify the difference in the hematopoietic microenvironment between Prx1-Cre;Hif-2α$^{fl/fl}$ mice and Hif-2α$^{fl/fl}$ mice, mice received two different interventions (including semilethal irradiation and 5-FU injection), and hematopoietic differences were evaluated. First, we observed hematopoietic changes after BM injury induced by semilethal irradiation. First, we collected PB from Prx1-Cre;Hif-2α$^{fl/fl}$ mice and Hif-2α$^{fl/fl}$ mice, and blood analysis indicated that beginning at the third week after irradiation, the recovery of WBCs (Figure 5A) and NEUs (Figure 5B) in Prx1-Cre;Hif-2α$^{fl/fl}$ mice was significantly slower than that in Hif-2α$^{fl/fl}$ mice. However, there were no statistically significant differences in HGB concentration (Figure 5C) or PLT count (Figure 5D) between Prx1-Cre;Hif-2α$^{fl/fl}$ mice and Hif-2α$^{fl/fl}$ mice.

Moreover, the HSCs and HPCs of Hif-2α$^{fl/fl}$ and Prx1-Cre;Hif-2α$^{fl/fl}$ mice were analyzed during the second week after semilethal irradiation. The results suggested that there was no significant difference in the TNC number (Figure 5E). Then, we analyzed the total number (Figure 5G) and proportion (Figure 5F) of HSCs and HPCs (Figure 5H and I) between the two genotypes of mice. There were no significant differences.

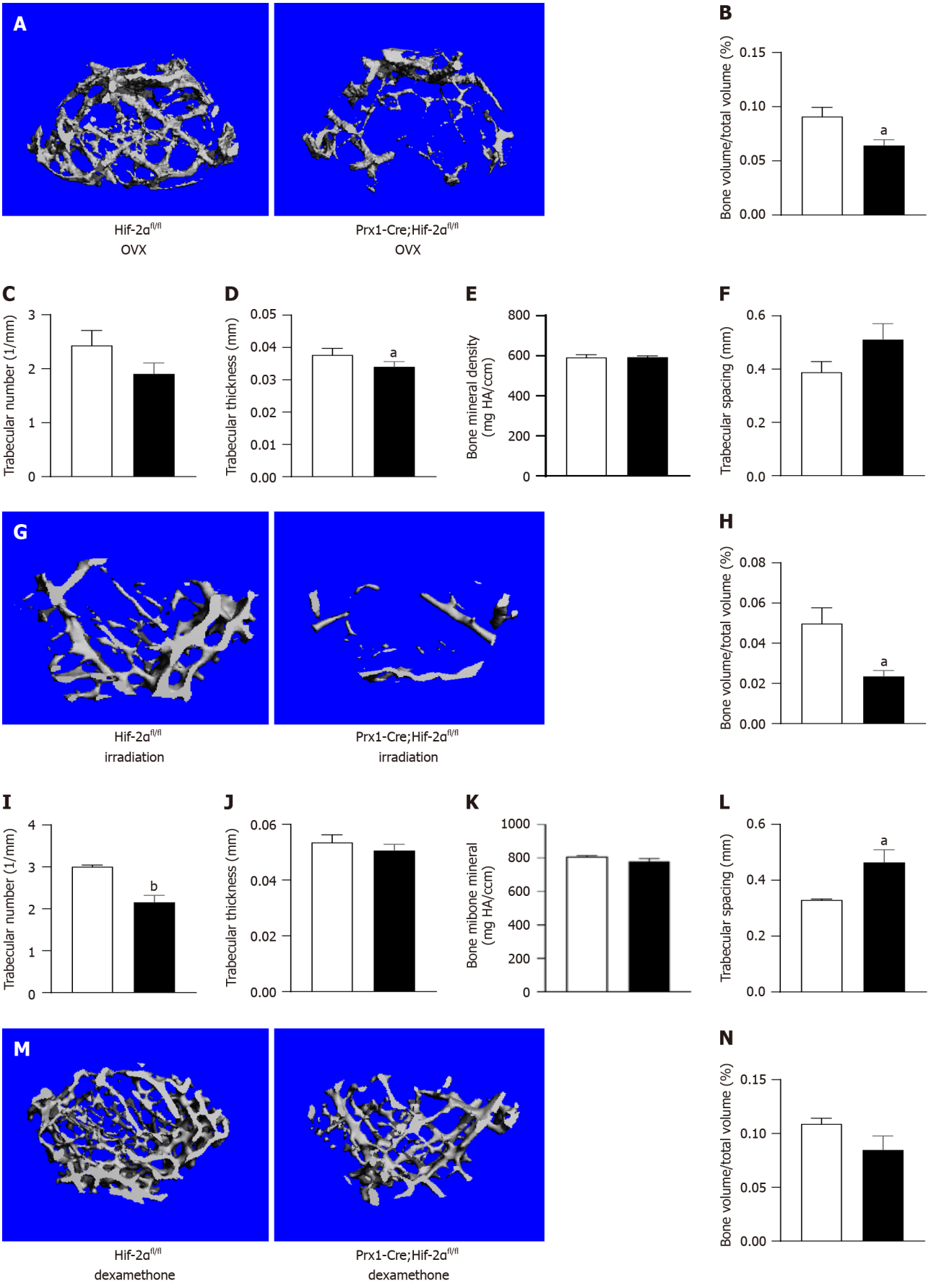
A
Hif-2α^fl/fl
OVX
Prx1-Cre;Hif-2α^fl/fl
OVX
B
Bone volume/total volume (%)
0.15
0.10
0.05
0.00
a
C
Trabecular number (1/mm)
3
2
1
0
D
Trabecular thickness (mm)
0.05
0.04
0.03
0.02
0.01
0.00
a
E
Bone mineral density (mg HA/ccm)
800
600
400
200
0
F
Trabecular spacing (mm)
0.6
0.4
0.2
0.0
G
Hif-2α^fl/fl
irradiation
Prx1-Cre;Hif-2α^fl/fl
irradiation
H
Bone volume/total volume (%)
0.08
0.06
0.04
0.02
0.00
a
I
Trabecular number (1/mm)
4
3
2
1
0
b
J
Trabecular thickness (mm)
0.06
0.04
0.02
0.00
K
Bone mibone mineral (mg HA/ccm)
1000
800
600
400
200
0
L
Trabecular spacing (mm)
0.6
0.4
0.2
0.0
a
M
Hif-2α^fl/fl
dexamethone
Prx1-Cre;Hif-2α^fl/fl
dexamethone
N
Bone volume/total volume (%)
0.15
0.10
0.05
0.00

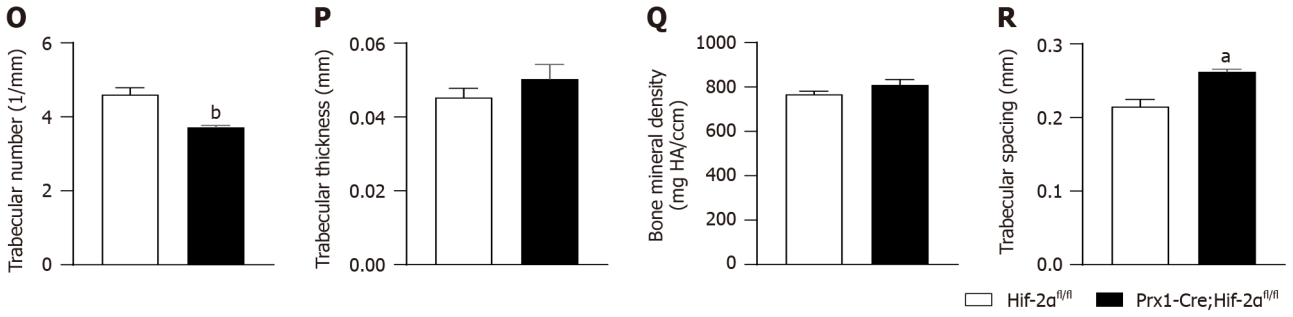

Figure 4 Adult Prx1-Cre;Hif-2α$^{fl/fl}$ and Hif-2α$^{fl/fl}$ mice exhibit decreased bone mass under three different stimulation conditions. A: Representative microcomputed tomography (μCT) images of femora from both Prx1-Cre;Hif-2α$^{fl/fl}$ and Hif-2α$^{fl/fl}$ mice 8 wk after ovariectomy; B-E: The bone volume (BV) fraction [BV/total volume (TV)] (B), trabecular number (Tb.N) (C), trabecular thickness (Tb.Th) (D) and bone mineral density (E) in the distal metaphysis of the femur were decreased by ovariectomy in Prx1-Cre;Hif-2α$^{fl/fl}$ mice, while the trabecular spacing (Tb.Sp) was appreciably increased in Prx1-Cre;Hif-2α$^{fl/fl}$ mice; G: Representative μCT images of femora from both Prx1-Cre;Hif-2α$^{fl/fl}$ and Hif-2α$^{fl/fl}$ mice 4 wk after semilethal irradiation; H-L: The BV/TV (H), Tb.N (I), Tb.Th (J) and BMD (K) in the distal metaphysis of the femur were obviously decreased by semilethal irradiation in Prx1-Cre;Hif-2α$^{fl/fl}$ mice, while the Tb.Sp (L) was appreciably increased in Prx1-Cre;Hif-2α$^{fl/fl}$ mice; M: Representative μCT images of femora from both Prx1-Cre;Hif-2α$^{fl/fl}$ and Hif-2α$^{fl/fl}$ mice 4 wk after dexamethasone treatment; N-R: The BV/TV (N), Tb.N (O), Tb.Th (P) and BMD (Q) in the distal metaphysis of the femur were obviously decreased by dexamethasone treatment in Prx1-Cre;Hif-2α$^{fl/fl}$ mice, while the Tb.Sp (R) was appreciably increased in Prx1-Cre;Hif-2α$^{fl/fl}$ mice. $^{a}P < 0.05$, $^{b}P < 0.01$.

We subsequently administered an intervention that caused BM injury in mice, *i.e.*, intraperitoneal injection of 5-FU, and then analyzed HSCs and HPCs in the BM of Prx1-Cre;Hif-2α$^{fl/fl}$ mice and Hif-2α$^{fl/fl}$ mice. The results still indicated that there was no significant difference in the number of TNCs in Prx1-Cre;Hif-2α$^{fl/fl}$ mice compared with Hif-2α$^{fl/fl}$ mice (Figure 5J). We subsequently analyzed the total number and proportion of HSCs and HPCs in the two genotypes of mice, and we found that the total number of HSCs (as shown in Figure 5L), the proportion of HSCs (as shown in Figure 5K), the total number of HPCs (as shown in Figure 5N) and the proportion of HPCs (as shown in Figure 5M) in Prx1-Cre;Hif-2α$^{fl/fl}$ mice did not significantly differ from those in Hif-2α$^{fl/fl}$ mice. Combined with the results of analysis of the hematopoietic phenotypes of the two mouse genotypes after irradiation, these results suggested that the hematopoietic recovery ability of Prx1-Cre;Hif-2α$^{fl/fl}$ mice after BM injury was not significantly different from that of Hif-2α$^{fl/fl}$ mice.

HIF-2α promoted the osteogenic differentiation and inhibited the adipogenic differentiation of BMSCs in vitro

BMSCs from Prx1-Cre;Hif-2α$^{fl/fl}$ mice and Hif-2α$^{fl/fl}$ mice were isolated to evaluate the fibroblast colony formation ability of the BMSCs and determine their proliferation ability. There was no difference in the CFU-F between Prx1-Cre;Hif-2α$^{fl/fl}$ and Hif-2α$^{fl/fl}$ mice. Representative images of CFU-Fs in Prx1-Cre;Hif-2α$^{fl/fl}$ and Hif-2α$^{fl/fl}$ mice are shown in Figure 6A. The quantification of the CFU-Fs formed by the BMSCs is shown in Figure 6B.

Because of the long duration of cell differentiation, there were no differences in the percentages of BMSCs isolated from Prx1-Cre;Hif-2α$^{fl/fl}$ and Hif-2α$^{fl/fl}$ mice before compared with after the interventions (bilateral ovariectomy, sublethal irradiation, or DEX treatment); therefore, in the remaining studies, we used BMSCs from naive mice. Hif-2α$^{fl/fl}$ mouse BMSCs were cultured and divided into the roxadustat and control groups according to whether they were treated with the HIF-2α agonist roxadustat. After 7 d of adipogenic differentiation, the adipogenic capacity of the roxadustat group was decreased. Oil red O staining indicated that the number of lipid droplets in the BMSCs of the roxadustat group was lower than that in the control group (Figure 6D), and quantification of oil red O staining indicated that lipid droplet formation was reduced in the BMSCs of the roxadustat group (Figure 6C). qPCR analysis revealed that roxadustat treatment significantly downregulated adipogenesis-related genes, such as Lpl (Figure 6E), adiponectin (Figure 6F) and CEBPa (Figure 6G), in BMSCs. These results suggest that activation of HIF-2α can reduce the adipogenic differentiation capacity of BMSCs.

After 14 d of osteogenic differentiation, the osteogenic differentiation capacity of the BMSCs in the roxadustat group was increased. Alizarin red staining indicated that the osteogenic differentiation capacity of the roxadustat group was increased compared with that of the control group (Figure 6I). Similarly, compared with those in the control group, the mRNA levels of osteogenesis-related genes, such as OCN (Figure 6H), Runx2 (Figure 6J) and Col1α1 (Figure 6K), were significantly increased in the roxadustat group. These results suggest that activation of HIF-2α can lead to an increased osteogenic differentiation capacity of BMSCs.

HIF-2α regulated adipogenesis and osteogenesis by inhibiting the mTOR pathway

To further investigate whether HIF-2α affects the osteogenic/adipogenic differentiation of BMSCs through the mTOR signaling pathway, we extracted protein and mRNA from BMSCs in the roxadustat group and the control group after adipogenic differentiation. The results suggested that, during the process of adipogenic differentiation, at the translational level, the levels of the key proteins of the mTOR signaling pathway - the p-mTOR protein and the downstream proteins p-PI3K and p-AKT (as shown in Figure 6M) - were significantly reduced in the roxadustat group (Figure 6L). Moreover, the mTOR activator MHY1485 was used to verify whether it could rescue the decreased adipogenic differentiation capacity of BMSCs. The results proved that the mTOR activator MHY1485 increased adipogenic capacity of BMSCs (Figure 7A and B) and the mRNA levels of the mTOR signaling pathway components (Figure 7C). Moreover, the protein levels of the mTOR signaling pathway components were increased (Figure 6L and M).

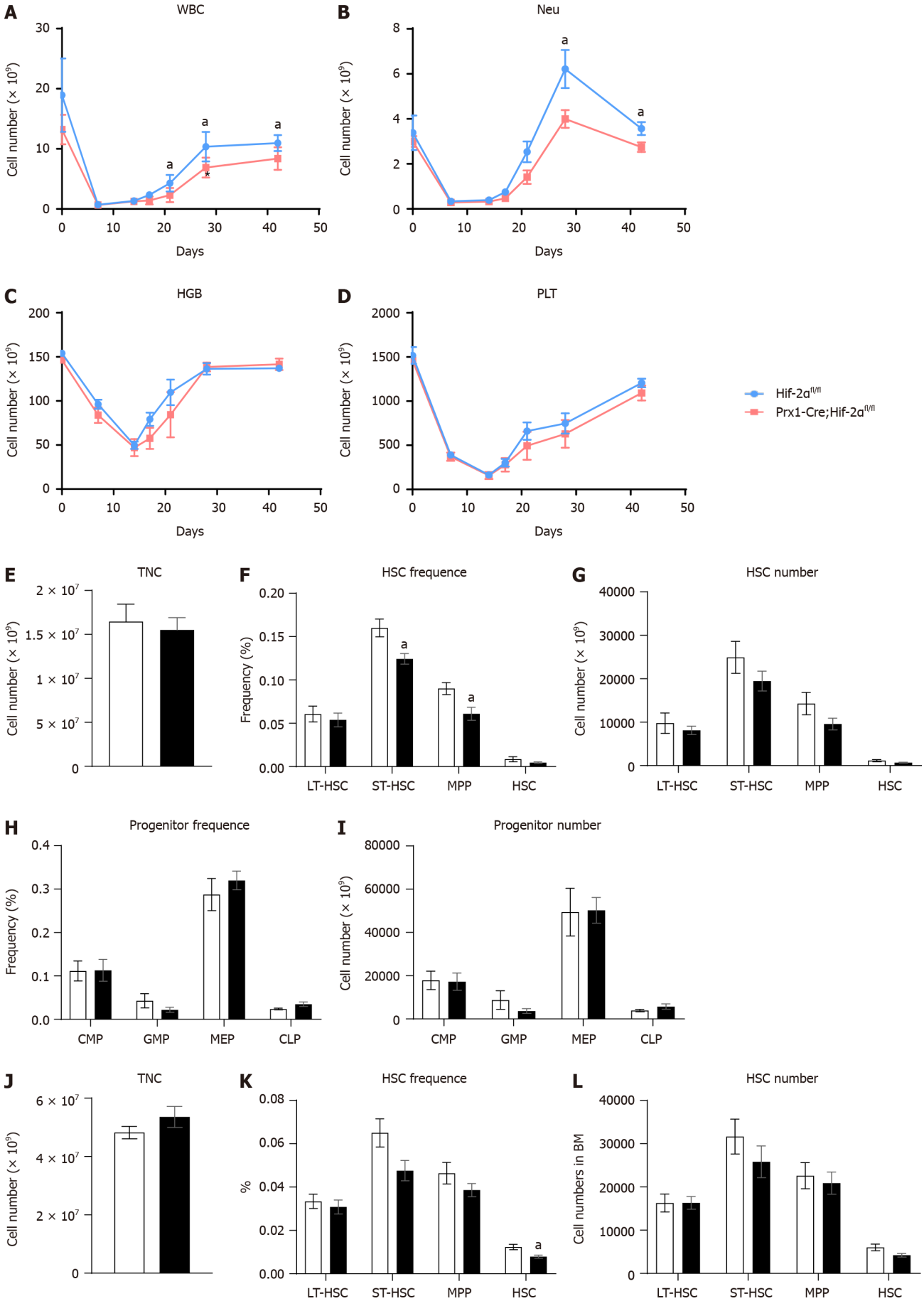
A
WBC
Cell number (× 10⁹)
Days
B
Neu
Cell number (× 10⁹)
Days
C
HGB
Cell number (× 10⁹)
Days
D
PLT
Cell number (× 10⁹)
Days
Hif-2α^fl/fl
Prx1-Cre;Hif-2α^fl/fl
E
TNC
Cell number (× 10⁹)
F
HSC frequence
Frequency (%)
LT-HSC
ST-HSC
MPP
HSC
G
HSC number
Cell number (× 10⁹)
LT-HSC
ST-HSC
MPP
HSC
H
Progenitor frequence
Frequency (%)
CMP
GMP
MEP
CLP
I
Progenitor number
Cell number (× 10⁹)
CMP
GMP
MEP
CLP
J
TNC
Cell number (× 10⁹)
K
HSC frequence
%
LT-HSC
ST-HSC
MPP
HSC
L
HSC number
Cell numbers in BM
LT-HSC
ST-HSC
MPP
HSC

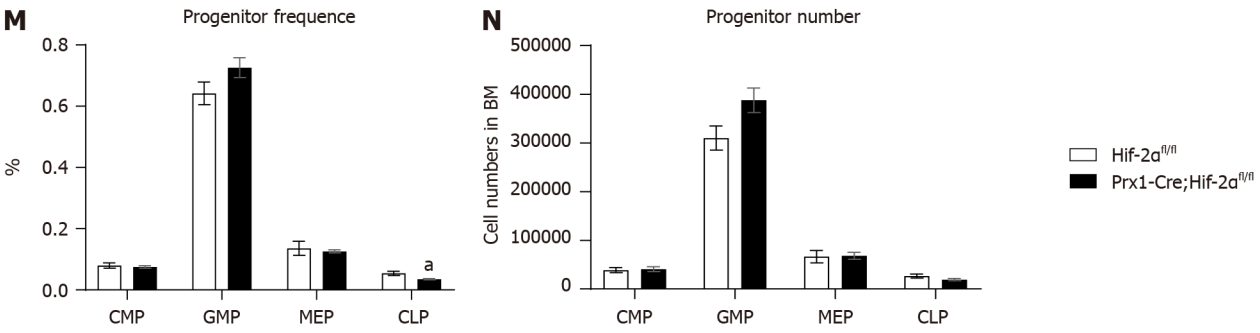

Figure 5 Adult Prx1-Cre;Hif-2α$^{fl/fl}$ and Hif-2α$^{fl/fl}$ mice exhibit normal hematopoiesis under different stimulation conditions. A-I: Eight-week-old Prx1-Cre;Hif-2α$^{fl/fl}$ and Hif-2α$^{fl/fl}$ mice were subjected to semilethal irradiation. The white blood cell count (A), red blood cell count (B), hemoglobin content (C) and platelet count (D) in peripheral blood were determined. Four weeks after semilethal irradiation, bone marrow (BM) cells freshly harvested from 8-wk-old Prx1-Cre;Hif-2α$^{fl/fl}$ and Hif-2α$^{fl/fl}$ mice were assayed by multiparameter fluorescence-activated cell sorting (FACS) analyses to determine the total nucleated cell (TNC) numbers (E), frequencies of hematopoietic stem cells (HSCs) (F), HSC numbers (G), frequencies of progenitors (H), and progenitor numbers (I); 8-wk-old Prx1-Cre;Hif-2α$^{fl/fl}$ and Hif-2α$^{fl/fl}$ mice were treated with 5-fluorouracil (5-FU); J-N: Four weeks after the 5-FU treatment regimen, BM cells freshly harvested from 8-wk-old Prx1-Cre;Hif-2α$^{fl/fl}$ and Hif-2α$^{fl/fl}$ mice were assayed *via* multiparameter FACS analyses to determine the TNC numbers (J), frequencies of HSCs (K), HSC numbers (L), frequencies of progenitors (M), and progenitor numbers (N). $^{a}P < 0.05$. WBC: White blood cell; NEU: Neutrophil; HGB: Hemoglobin; PLT: Platelet; TNC: Total nucleated cell; HSC: Hematopoietic stem cell; LT-HSC: Long-term hematopoietic stem cell; ST-HSC: Short-term hematopoietic stem cell; MPP: Multipotent progenitor; CMP: Common myeloid progenitor; GMP: Granulocyte-monocyte progenitor; MEP: Megakaryocyte-erythroid progenitor; CLP: Common lymphoid progenitor; HIF-2α: Hypoxia-inducible factor 2alpha.

On the other hand, we used the HIF-2α inhibitor PT2399 and the mTOR inhibitor rapamycin to confirm that HIF-2α regulates adipogenesis by inhibiting the mTOR pathway. We divided cultured BMSCs into three different groups: The control group, the PT2399 group, and the PT2399 + rapamycin group. The results showed that the PT2399 + rapamycin treatment group exhibited a decreased adipogenic differentiation capacity, which was increased in the PT2399 group. Oil red O staining and quantitative analysis indicated that lipid droplet formation was increased in the PT2399-treated BMSCs (Figure 7F), and that after BMSCs were treated with PT2399 and rapamycin, their adipogenic differentiation capacity decreased. At the transcriptional level, the expression levels of genes related to adipogenesis in BMSCs were significantly upregulated in the PT2399 group and downregulated in the PT2399 + rapamycin group (Figure 7D). Similarly, the expression of key mRNAs in the mTOR signaling pathway was significantly decreased in the PT2399 + rapamycin group compared to the PT2399 group (Figure 7E). Then, we extracted protein from BMSCs in the PT2399 group and the PT2399 + rapamycin group after adipogenic differentiation. The results suggested that, during the process of adipogenic differentiation, the levels of the mTOR and p-mTOR proteins and the downstream proteins PI3K, p-PI3K and p-AKT (as shown in Figure 7H) were significantly increased in the PT2399 group but decreased in the PT2399 + rapamycin group (Figure 7G).

Furthermore, we verified the relevant results regarding the osteogenic differentiation of BMSCs using the HIF-2α inhibitor PT2399 and the mTOR inhibitor rapamycin. Similarly, we divided the cultured BMSCs into three different groups: The control group, the PT2399 group, and the PT2399 + rapamycin group. The results showed that rapamycin rescued the decreased osteogenic differentiation ability of the PT2399 group. Alizarin red staining was used to quantify the osteogenic differentiation capacity of the cells, and the results indicated that the osteogenic differentiation capacity was decreased in the PT2399 group (Figure 8A); moreover, for the in BMSCs treated with PT2399 and rapamycin, the osteogenic differentiation capacity was increased. At the transcriptional level, the expression of genes related to osteogenesis in BMSCs, such as OCN (Figure 8B), RUNX2 (Figure 8C) and Col1α1 (Figure 8D), was significantly downregulated in the PT2399 group and upregulated in the PT2399 + rapamycin group. Then, after osteogenic differentiation, we extracted protein from the BMSCs in the PT2399 group and the PT2399 + rapamycin group. The results suggested that, during the process of osteogenic differentiation, the levels of the mTOR and p-mTOR proteins and the downstream proteins PI3K, p-PI3K, p-AKT and AKT (as shown in Figure 8E) were significantly increased in the PT2399 group but decreased in the PT2399 + rapamycin group (Figure 8F).

DISCUSSION

We successfully generated mice with BMSC-specific HIF-2α knockout, which were used for our subsequent studies. Notably, during the process of generating the Prx1-Cre;Hif-2α$^{fl/fl}$ mice, we found that female mice harboring the Prx1-Cre gene could not be mated. Upon further investigation, we found that the birth rate of the mice was very low and that the stillbirth rate was high. We have not further clarified and studied the mechanism of this phenomenon, but upon observing this phenomenon, we avoided using females with the prx1-Cre transgene as for breeding; therefore, we expanded the mouse population by mating female Hif-2α$^{fl/fl}$ mice with male Prx1-Cre;Hif-2α$^{fl/fl}$ mice. This phenomenon has not been explained by the relevant literature in other studies and could be investigated in our future research.

Many studies have explored the role of HIF-1α in bone homeostasis and have shown that HIF-1α can promote osteogenesis. It was reported that mice lacking Hif-1α exhibited a significant reduction in trabecular BV, a reduced bone

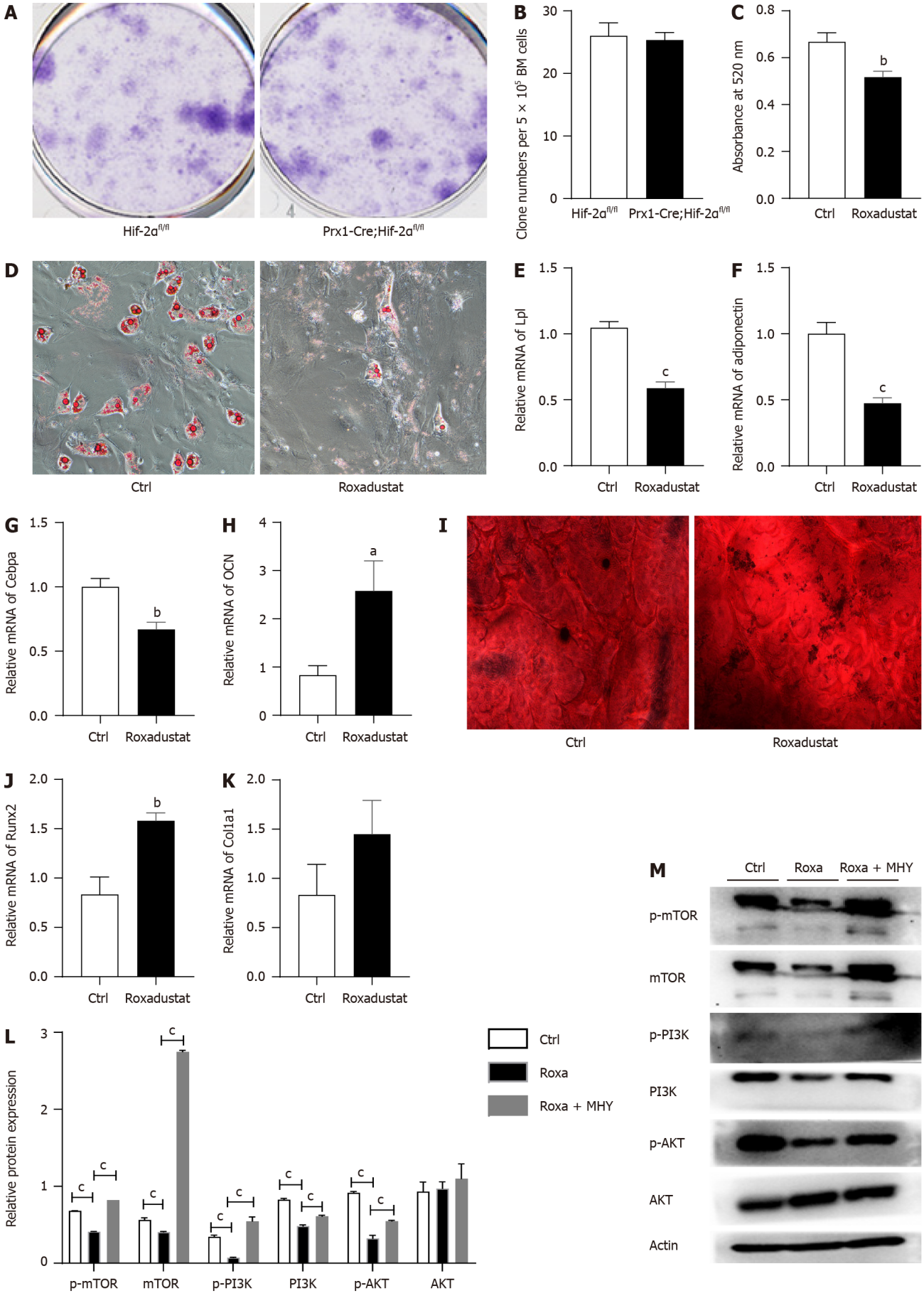

Figure 6 Treatment with the hypoxia-inducible factor 2alpha agonist roxadustat increases osteogenesis and decreases adipogenesis. A:

Representative images of the fibroblast colony-forming unit (CFU-F) assay with Prx1-Cre;Hif-2α$^{fl/fl}$ and Hif-2α$^{fl/fl}$ mice are shown; B: Quantification of CFU-Fs formed by bone mesenchymal stem cells (BMSCs) from Prx1-Cre;Hif-2α$^{fl/fl}$ and Hif-2α$^{fl/fl}$ mice are shown; C and D: Hif-2α$^{fl/fl}$ mouse BMSCs were cultured with or without roxadustat. In the adipogenic differentiation assay, Oil red O staining was performed after seven days (D); quantification of Oil Red O staining in BMSCs after induction of adipogenic differentiation (C); E-M: Relative mRNA levels of the adipogenesis-related genes Lpl (E), Adiponectin (F) and Cebpa (G) in BMSCs after 7 d of adipogenic differentiation. In the osteogenic differentiation assay, Alizarin red staining was performed after 14 d to quantify osteoblast mineralization (I). Relative mRNA levels of the osteogenesis-related genes OCN (H), Runx2 (J) and Col1α1 (K) in BMSCs after 14 d of osteogenic differentiation. Adipogenic differentiation was induced in BMSCs by treatment with roxadustat and MHY1485 for 7 d. The levels of the mechanistic target of rapamycin (mTOR) and PI3K/AKT signaling pathway proteins were measured *via* western blotting in the Ctrl, roxadustat and Roxadustat + MHY1485 groups (M). Quantification of the relative levels of the mTOR, PI3K and AKT proteins (L). The phosphorylated protein levels were normalized to the corresponding total protein levels. $^{a}P < 0.05$, $^{b}P < 0.01$, $^{c}P < 0.001$. Roxa: Roxadustat; MHY: MHY1485; HIF-2α: Hypoxia-inducible factor 2alpha; mTOR: Mechanistic target of rapamycin.

formation rate, and altered cortical bone architecture. In contrast, mice lacking HIF-2α had only a modest decrease in trabecular BV[21]. It has also been suggested that HIF-1α stabilization in osteoblast precursors of postnatal mice markedly increases the osteoblast number and bone mass[22]. Recently, several studies have demonstrated that HIF-2α is involved in BMSC osteogenic differentiation. However, the molecular mechanism and role of HIF-2α in hematopoietic function in the BM niche have not been determined. Although the two α subunits are structurally similar and recognize the same DNA elements, the target genes regulated by HIF-1α and HIF-2α are not identical. Cheng *et al*[23] generated conditional Phd2 knockout (cKO) mice from osteoblast lineage cells by crossing floxed Phd2 mice with a Col1α2-i Cre line to investigate the function of Phd2 *in vivo*. The cKO mice developed short stature and experienced premature death at 12 to 14 wk of age. Compared to WT mice, cKO mice had a reduced bone mineral content, bone area, and BMD in the femora and tibiae but not in the vertebrae. The TV, BV and BV fraction (BV/TV) of femoral trabeculae in cKO mice were significantly decreased[23]. A recent study by Lee *et al*[24] suggested that HIF-2α deficiency promoted osteoblast differentiation and inhibited osteoclast differentiation by increasing bone mass. Merceron *et al*[25] demonstrated that HIF-2α is an inhibitor of osteoblast formation and increased bone mass. Guo *et al*[26] conditionally knocked out HIF-2α in leptin receptor-expressing cells and their progeny in mice and found that radiation therapy in littermate control mice reduced bone mass, but HIF-2α conditional knockout mice maintained a bone mass comparable to that of nonirradiated control animals.

Taken together, our findings in this study support the role of HIF-2α in promoting osteogenesis, especially in combination with interventions such as bilateral ovariectomy, semilethal irradiation, and DEX treatment. Moreover, the Prx1-Cre;Hif-2α$^{fl/fl}$ phenotype did not significantly differ in terms of BMD in mice under the naive condition, but the BMD in mice subjected to the various stimulation interventions was indicative of a significant decrease in osteogenesis in Prx1-Cre;Hif-2α$^{fl/fl}$ mice. We hypothesized that the concentration of HIF-2α in the BM of mice under stress stimulation was elevated, leading to an alteration in BMD in these mice. Our results are consistent with those of previous studies. Shomento *et al*[21] used Osteocalcin-Cre mice and HIF-2α Flox mice to generate mice with osteoblast-specific HIF-2α knockout, and the results suggested that KO mice had reduced BMD. Wu *et al*[27] selected osx-cre-labeled osteoblasts and PHD mutant mice to generate mice with osteoblast-specific PHD knockout, which exhibited increased BMD. Wang *et al*[28] overexpressed HIFα in osteoblasts of mice by selective deletion of the Vhl, resulting in increased BMD.

Taken together, our results suggest that HIF-2α deletion in the BM microenvironment does not significantly affect HSC or HPC function in mice. These results indicate that the HIF-2α gene in the BM microenvironment does not affect the stromal niche of HSCs, only bone formation. Our results are consistent with those of previous studies. Wu *et al*[27] selected Osx-cre-labeled osteoblasts and PHD mutant mice to generate mice with osteoblast-specific PHD knockout (KO). The KO mice exhibited increased BMD without disruption of hematopoietic homeostasis[27]. However, notably, although the deletion of HIF-2α had no significant effect on HSC function, PB analysis revealed that the hemoglobin content and hematocrit value were significantly lower in Prx1-Cre;Hif-2α$^{fl/fl}$ mice than in WT mice, suggesting that other mechanisms may lead to the decreased hemoglobin content observed in Prx1-Cre;Hif-2α$^{fl/fl}$ mice. Rankin *et al*[29] reported that pharmacological or genetic inhibition of prolyl hydroxylases 1/2/3 in osteoprogenitors elevated EPO expression in bone and increased the hematocrit value, an effect believed to be caused by increased EPO expression and modulation of erythropoiesis in osteoblasts. Our results are consistent with the above results. Therefore, to further study the causes of the decreased hemoglobin content in Prx1-Cre;Hif-2α$^{fl/fl}$ mice observed in this study, further studies can be carried out focusing on EPO.

Recently, accumulating evidence has highlighted the role of mTOR signaling in regulating bone homeostasis, which provides insight into the pathogenesis of OP. It is widely believed that the inhibition of mTOR signaling can promote osteoblastic differentiation, but this remains a controversial issue[30]. Rapamycin is an inhibitor of mTOR signaling, and a high-throughput screening assay showed that rapamycin can promote osteoblastic differentiation-treatment of osteoblast precursors with rapamycin alone or in combination with bone morphogenetic protein (BMP)-2 increased the levels of the phospho-Smad 1/5/8 proteins and the transcription of Runx-2, Osx and Smad-7, consistent with a role in promoting osteoblastic differentiation[31]. Moreover, rapamycin effectively stimulates the osteoblastic differentiation of human embryonic stem cells by inhibiting rapamycin-sensitive mTOR signaling and promoting BMP/Smad signaling[32]. Similarly, blockade of mTOR signaling by osteoblast-specific knockout or rapamycin treatment rescues the osteopenia phenotype in fibrillin-1-deficient mice by augmenting the osteogenic differentiation and inhibiting the adipogenic differentiation of BMSCs[33]. These findings are consistent with the above results, suggesting that the activation of HIF-2α in BMSCs inhibits the mTOR signaling pathway, resulting in a reduction in the adipogenic differentiation and an increase in the osteogenic differentiation of BMSCs. Therefore, we believe that HIF-2α inhibits adipogenic differentiation and promotes osteogenesis by inhibiting the mTOR signaling pathway.

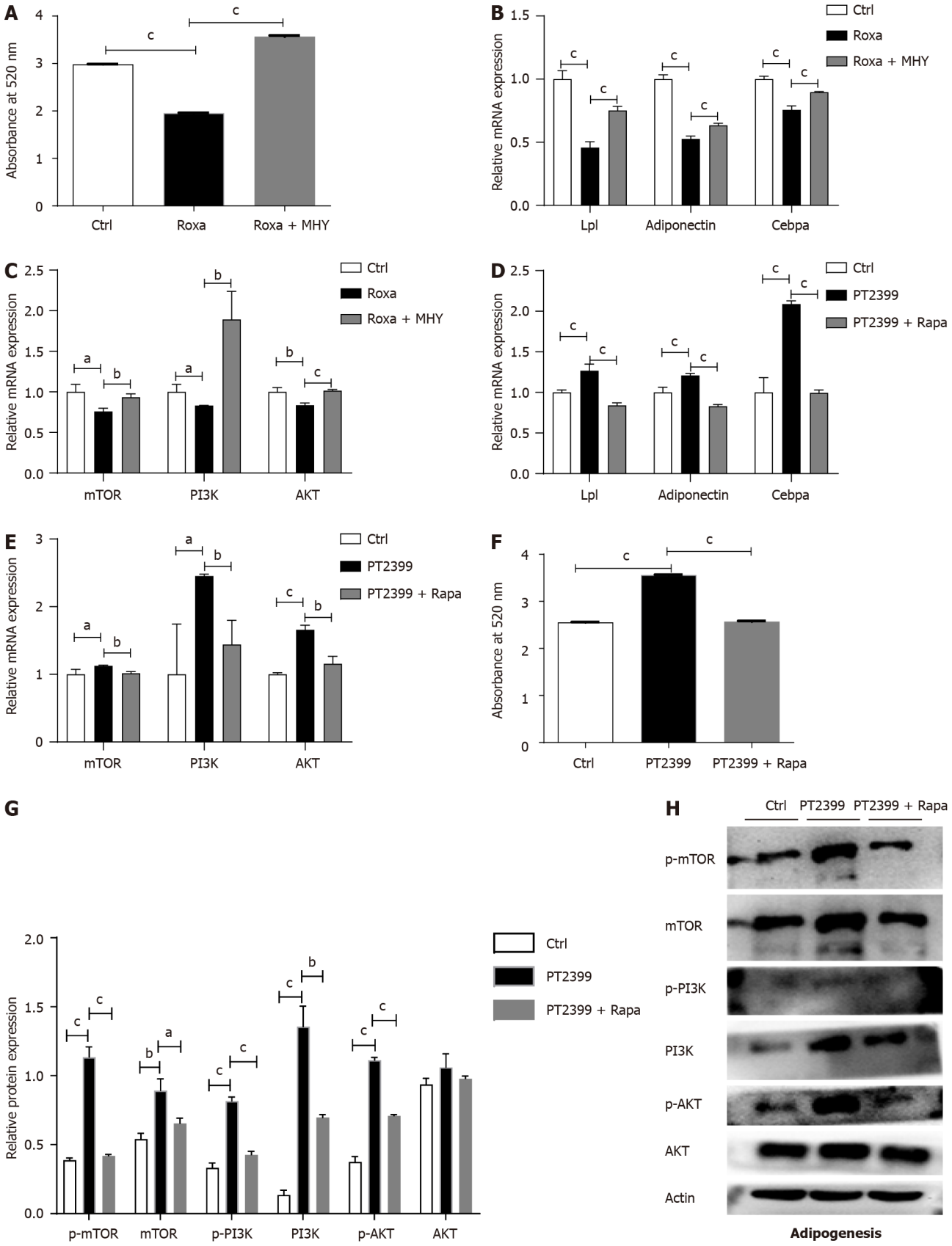

Figure 7 Hypoxia-inducible factor 2alpha decreases bone mesenchymal stem cell adipogenic differentiation by inhibiting mechanistic target of rapamycin and PI3K/AKT signaling. Adipogenic differentiation was induced in Hif-2α$^{fl/fl}$ bone mesenchymal stem cells (BMSCs) by treatment with roxadustat and MHY1485 for 7 d. A: Quantification of Oil Red O staining in BMSCs after induction of adipogenic differentiation; B: Relative mRNA expression levels of the adipogenesis-related genes Lpl, Adiponectin and Cebpα in BMSCs during adipogenic differentiation; C-G:: Relative mRNA expression levels of the mechanistic target of rapamycin (mTOR) signaling-related genes mTOR, PI3K and AKT in BMSCs during adipogenic differentiation (C) Adipogenic differentiation was induced in BMSCs by treatment with 10 μM PT2399 and 100 nM rapamycin for 7 d; quantification of Oil Red O staining in BMSCs after induction of adipogenic differentiation (F);

relative mRNA expression levels of adipogenesis-related genes in BMSCs with induction of osteogenic differentiation with PT2399 and the mTOR inhibitor rapamycin (D). Relative mRNA expression levels of mTOR signaling-related genes in BMSCs with induction of adipogenic differentiation with PT2399 and rapamycin (E). Protein levels were measured by western blotting in the PT2399 and PT2399 + rapamycin groups (H). Quantification of the relative p-mTOR, mTOR, p-PI3K, PI3K, p-AKT and AKT levels. The phosphorylated protein levels were normalized to the corresponding total protein levels (G). $^{a}P < 0.05$, $^{b}P < 0.01$, $^{c}P < 0.001$. Roxa: roxadustat, MHY: MHY1485, Rapa: Rapamycin; mTOR: Mechanistic target of rapamycin.

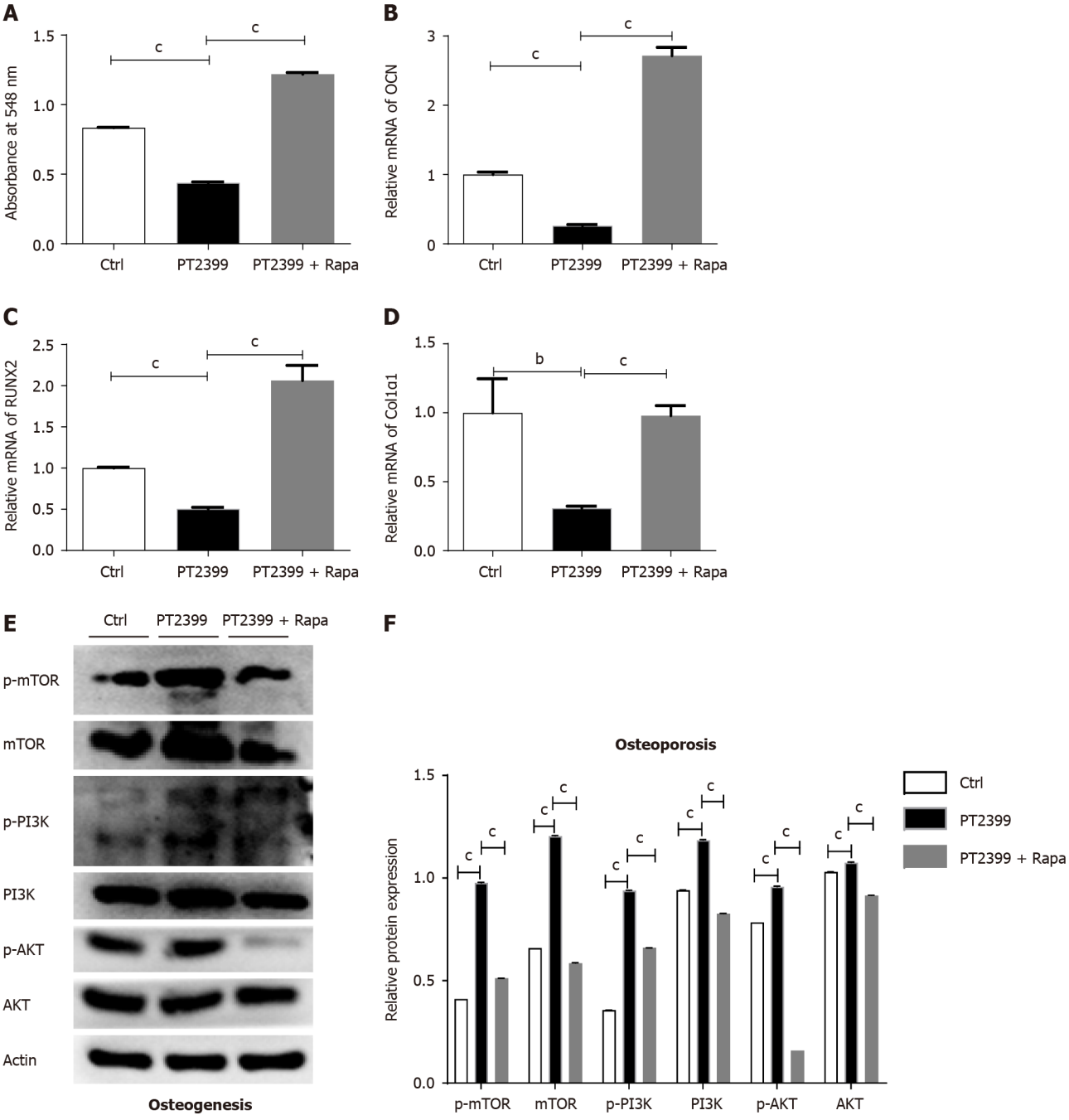

Figure 8 The mechanistic target of rapamycin inhibitor rapamycin rescued the decrease in the osteogenic differentiation of bone mesenchymal stem cells induced by the hypoxia-inducible factor 2alpha inhibitor PT2399. A-F: Osteogenic differentiation was induced in Hif-2α$^{fl/fl}$ bone mesenchymal stem cells (BMSCs) by treatment with 10 μM PT2399 and 100 nM rapamycin for 14 d: Quantification of alizarin red staining in BMSCs after induction of osteogenic differentiation (A); relative mRNA expression levels of the osteogenesis-related genes OCN (B), RUNX2 (C) and Col1α1 (D) in BMSCs cells with induction of osteogenic differentiation with PT2399 and the mechanistic target of rapamycin (mTOR) inhibitor rapamycin. Protein levels were measured by western blotting in the PT2399 and PT2399 + rapamycin groups (E). Quantification of the relative p-mTOR, mTOR, p-PI3K, PI3K, p-AKT and AKT levels (F). The phosphorylated protein levels were normalized to the corresponding total protein levels. $^{b}P < 0.01$, $^{c}P < 0.001$. Rapa: Rapamycin; mTOR: Mechanistic target of rapamycin.

Under physiological conditions, HIF-2α is hydroxylated by the PHD protein, leading to Vhl-dependent ubiquitination and protease-dependent degradation[34]. Therefore, the PHD inhibitor roxadustat (FG-4592) activates HIF-2α by increasing HIF-2α stability[35]. The drug is currently on the market in China and is approved for the treatment of renal anemia. In addition, several randomized phase II and III trials have shown that roxadustat significantly reduces plasma total cholesterol levels in patients with chronic kidney disease[36-38]. Moreover, roxadustat has potential use as an antiatherosclerotic treatment. Several studies have shown that roxadustat has an inhibitory effect on obesity-induced atherosclerosis, which depends primarily on the regulation of HIF-2α and ceramide metabolism in adipocytes[39]. In addition to its use for treating CKD-related anemia, roxadustat is potentially useful for the treatment of carcinoma, neurological diseases, ocular diseases, tissue injuries, and obesity[40]. However, studies on roxadustat and osteogenesis are rare. Roxadustat has been suggested to promote fracture repair *in vivo* by increasing the number of BMSCs and promoting chondrogenesis. *In vitro*, roxadustat significantly improved BMSC proliferation and migration by increasing the concentrations of intracellular calcium ions and NO and simultaneously decreasing the level of reactive oxygen species[41]. Hulley *et al*[42] suggested that roxadustat could inhibit osteoclast activity and subsequent bone resorption after coculture with osteoblasts. Our *in vitro* experiments revealed that roxadustat could promote the osteogenic differentiation of BMSCs and suggested that roxadustat might have a therapeutic effect on promoting osteogenesis in the context of OP. More studies could be carried out to verify the above speculation.

This study has several limitations. We have not verified the effect of HIF-2α on osteoclasts. Since bone homeostasis is a balance between osteoblast and osteoclast activity, the relationship between osteogenesis and osteoclasia should be assessed while observing the phenotype of bone, which is also the focus of our next study.

CONCLUSION

In conclusion, through *in vivo* and *in vitro* experiments, we verified that HIF-2α promoted the osteogenic differentiation and inhibited the adipogenic differentiation of BMSCs by inhibiting the mTOR signaling pathway. Moreover, HIF-2α had no effect on the number or function of HSCs or HPCs in the BM microenvironment. *In vivo* experiments showed that OP in Prx1-Cre;Hif-2α$^{fl/fl}$ mice was aggravated by bilateral ovariectomy, sublethal irradiation, and DEX treatment. Through *in vitro* experiments, it was confirmed that HIF-2α can inhibit the mTOR signaling pathway, leading to multiple factors, such as the promotion of BMSC osteogenic differentiation, inhibition of BMSC adipogenic differentiation, inhibition of erythropoiesis, and promotion of the anti-injury function of WBCs to regulate the BM niche, thus participating in the occurrence and progression of OP.

ARTICLE HIGHLIGHTS

Research background

Recently, several studies have demonstrated that hypoxia-inducible factor 2alpha (HIF-2α) is involved in bone mesenchymal stem cell (BMSC) osteogenic differentiation. However, the molecular mechanism involved remains unclear.

Research motivation

An exploration of osteoporosis (OP) treatments aimed at increasing bone formation is needed.

Research objectives

Research on the effects of HIF-2α on the osteogenic and adipogenic differentiation of BMSCs and hematopoietic function in the bone marrow niche.

Research methods

In vivo, we generated mice with BMSC-specific HIF-2α knockout and induced OP in these mice *via* three interventions: Bilateral ovariectomy, semilethal irradiation, and treatment with dexamethasone.

Research results

In vivo, the bone mass of KO mice was decreased compared with that of WT mice. *In vitro*, downregulation of HIF-2α inhibited osteogenesis and increased adipogenesis by suppressing the mechanistic target of rapamycin (mTOR) signaling pathway.

Research conclusions

In conclusion, through *in vivo* and *in vitro* experiments, we verified that inhibition of HIF-2α can decrease the osteogenic differentiation and increase the adipogenic differentiation of BMSCs by inhibiting the mTOR signaling pathway.

Research perspectives

In future research, as many patients with chronic kidney disease also have OP, we will verify whether the HIF-2α agonist roxadustat can successfully treat mice with OP induced *via* ovariectomy.

FOOTNOTES

Co-first authors: Ling-Ling Wang and Zhan-Jin Lu.

Author contributions: Wang LL and Lu ZJ contributed equally to this work; Wang LL and Lu HY are involved in study concept and design; Wang LL, Lu ZJ, Luo SK, Li Y, and Yang Z performed experiments; Luo SK, Li Y, and Yang Z provided material support and analytic tools; Wang LL, Lu ZJ, and Lu HY analyzed the data and wrote the manuscript; Lu HY had supervision of all study; and all authors read and approved the final manuscript.

Supported by Basic and Applied Basic Research Foundation of Guangdong Province, No. 2020A1515010123 and No. 2021A1515010695; and Special Fund Project for Science and Technology Innovation Strategy of Guangdong Province, No. 2019A030317011.

Institutional animal care and use committee statement: The study was reviewed and approved by the Animal Care and Ethics Committee of the Fifth Affiliated Hospital of Sun Yat-sen University (Animal protocol number: 00054).

Conflict-of-interest statement: All the authors report no relevant conflicts of interest for this article.

Data sharing statement: No additional data are available.

ARRIVE guidelines statement: The authors have read the ARRIVE guidelines, and the manuscript was prepared and revised according to the ARRIVE guidelines.

Country/Territory of origin: China

ORCID number: Ling-Ling Wang 0000-0001-8066-7638; Shun-Kui Luo 0000-0001-6252-1715; Hong-Yun Lu 0000-0001-8794-0887.

S-Editor: Wang JJ
L-Editor: A
P-Editor: Yuan YY

REFERENCES

1 **Fuggle NR**, Curtis EM, Ward KA, Harvey NC, Dennison EM, Cooper C. Fracture prediction, imaging and screening in osteoporosis. *Nat Rev Endocrinol* 2019; **15**: 535-547 [PMID: 31189982 DOI: 10.1038/s41574-019-0220-8]

2 **Wang L**, Yu W, Yin X, Cui L, Tang S, Jiang N, Zhao N, Lin Q, Chen L, Lin H, Jin X, Dong Z, Ren Z, Hou Z, Zhang Y, Zhong J, Cai S, Liu Y, Meng R, Deng Y, Ding X, Ma J, Xie Z, Shen L, Wu W, Zhang M, Ying Q, Zeng Y, Dong J, Cummings SR, Li Z, Xia W. Prevalence of Osteoporosis and Fracture in China: The China Osteoporosis Prevalence Study. *JAMA Netw Open* 2021; **4**: e2121106 [PMID: 34398202 DOI: 10.1001/jamanetworkopen.2021.21106]

3 **Tang L**, Wu M, Lu S, Zhang H, Shen Y, Shen C, Liang H, Ge H, Ding X, Wang Z. Fgf9 Negatively Regulates Bone Mass by Inhibiting Osteogenesis and Promoting Osteoclastogenesis Via MAPK and PI3K/AKT Signaling. *J Bone Miner Res* 2021; **36**: 779-791 [PMID: 33316109 DOI: 10.1002/jbmr.4230]

4 **Kiernan J**, Davies JE, Stanford WL. Concise Review: Musculoskeletal Stem Cells to Treat Age-Related Osteoporosis. *Stem Cells Transl Med* 2017; **6**: 1930-1939 [PMID: 28834263 DOI: 10.1002/sctm.17-0054]

5 **Wan Y**. Bone marrow mesenchymal stem cells: fat on and blast off by FGF21. *Int J Biochem Cell Biol* 2013; **45**: 546-549 [PMID: 23270727 DOI: 10.1016/j.biocel.2012.12.014]

6 **Spencer JA**, Ferraro F, Roussakis E, Klein A, Wu J, Runnels JM, Zaher W, Mortensen LJ, Alt C, Turcotte R, Yusuf R, Côté D, Vinogradov SA, Scadden DT, Lin CP. Direct measurement of local oxygen concentration in the bone marrow of live animals. *Nature* 2014; **508**: 269-273 [PMID: 24590072 DOI: 10.1038/nature13034]

7 **Lee KE**, Simon MC. From stem cells to cancer stem cells: HIF takes the stage. *Curr Opin Cell Biol* 2012; **24**: 232-235 [PMID: 22296771 DOI: 10.1016/j.ceb.2012.01.005]

8 **Yellowley CE**, Genetos DC. Hypoxia Signaling in the Skeleton: Implications for Bone Health. *Curr Osteoporos Rep* 2019; **17**: 26-35 [PMID: 30725321 DOI: 10.1007/s11914-019-00500-6]

9 **Mangiavini L**, Merceron C, Araldi E, Khatri R, Gerard-O'Riley R, Wilson TL, Rankin EB, Giaccia AJ, Schipani E. Loss of VHL in mesenchymal progenitors of the limb bud alters multiple steps of endochondral bone development. *Dev Biol* 2014; **393**: 124-136 [PMID: 24972088 DOI: 10.1016/j.ydbio.2014.06.013]

10 **Kaluz S**, Tan C, Van Meir EG. Taking a HIF pill for old age diseases? *Aging (Albany NY)* 2018; **10**: 290-292 [PMID: 29500331 DOI: 10.18632/aging.101395]

11 **Picke AK**, Campbell GM, Blüher M, Krügel U, Schmidt FN, Tsourdi E, Winzer M, Rauner M, Vukicevic V, Busse B, Salbach-Hirsch J, Tuckermann JP, Simon JC, Anderegg U, Hofbauer LC, Saalbach A. Thy-1 (CD90) promotes bone formation and protects against obesity. *Sci Transl Med* 2018; **10** [PMID: 30089635 DOI: 10.1126/scitranslmed.aao6806]

12 **Yue R**, Shen B, Morrison SJ. Clec11a/osteolectin is an osteogenic growth factor that promotes the maintenance of the adult skeleton. *Elife* 2016; **5** [PMID: 27976999 DOI: 10.7554/eLife.18782]

13 **Wenxi D**, Shufang D, Xiaoling Y, Liming Y. Panax notoginseng saponins suppress radiation-induced osteoporosis by regulating bone formation and resorption. *Phytomedicine* 2015; **22**: 813-819 [PMID: 26220628 DOI: 10.1016/j.phymed.2015.05.056]

14 **Ni F**, Yu WM, Wang X, Fay ME, Young KM, Qiu Y, Lam WA, Sulchek TA, Cheng T, Scadden DT, Qu CK. Ptpn21 Controls Hematopoietic Stem Cell Homeostasis and Biomechanics. *Cell Stem Cell* 2019; **24**: 608-620.e6 [PMID: 30880025 DOI: 10.1016/j.stem.2019.02.009]

15 **Suire C**, Brouard N, Hirschi K, Simmons PJ. Isolation of the stromal-vascular fraction of mouse bone marrow markedly enhances the yield of clonogenic stromal progenitors. *Blood* 2012; **119**: e86-e95 [PMID: 22262767 DOI: 10.1182/blood-2011-08-372334]

16 **Yin LM**, Jiang HF, Wang X, Qian XD, Gao RL, Lin XJ, Chen XH, Wang LC. Effects of sodium copper chlorophyllin on mesenchymal stem cell function in aplastic anemia mice. *Chin J Integr Med* 2013; **19**: 360-366 [PMID: 23001462 DOI: 10.1007/s11655-012-1210-z]

17 **Morikawa S**, Mabuchi Y, Kubota Y, Nagai Y, Niibe K, Hiratsu E, Suzuki S, Miyauchi-Hara C, Nagoshi N, Sunabori T, Shimmura S, Miyawaki A, Nakagawa T, Suda T, Okano H, Matsuzaki Y. Prospective identification, isolation, and systemic transplantation of multipotent mesenchymal stem cells in murine bone marrow. *J Exp Med* 2009; **206**: 2483-2496 [PMID: 19841085 DOI: 10.1084/jem.20091046]

18 **Pinho S**, Lacombe J, Hanoun M, Mizoguchi T, Bruns I, Kunisaki Y, Frenette PS. PDGFRα and CD51 mark human nestin+ sphere-forming mesenchymal stem cells capable of hematopoietic progenitor cell expansion. *J Exp Med* 2013; **210**: 1351-1367 [PMID: 23776077 DOI: 10.1084/jem.20122252]

19 **Li Y**, Fu H, Wang H, Luo S, Wang L, Chen J, Lu H. GLP-1 promotes osteogenic differentiation of human ADSCs *via* the Wnt/GSK-3β/β-catenin pathway. *Mol Cell Endocrinol* 2020; **515**: 110921 [PMID: 32615283 DOI: 10.1016/j.mce.2020.110921]

20 **Huebner AK**, Schinke T, Priemel M, Schilling S, Schilling AF, Emeson RB, Rueger JM, Amling M. Calcitonin deficiency in mice progressively results in high bone turnover. *J Bone Miner Res* 2006; **21**: 1924-1934 [PMID: 17002587 DOI: 10.1359/jbmr.060820]

21 **Shomento SH**, Wan C, Cao X, Faugere MC, Bouxsein ML, Clemens TL, Riddle RC. Hypoxia-inducible factors 1alpha and 2alpha exert both distinct and overlapping functions in long bone development. *J Cell Biochem* 2010; **109**: 196-204 [PMID: 19899108 DOI: 10.1002/jcb.22396]

22 **Regan JN**, Lim J, Shi Y, Joeng KS, Arbeit JM, Shohet RV, Long F. Up-regulation of glycolytic metabolism is required for HIF1α-driven bone formation. *Proc Natl Acad Sci U S A* 2014; **111**: 8673-8678 [PMID: 24912186 DOI: 10.1073/pnas.1324290111]

23 **Cheng S**, Xing W, Pourteymoor S, Mohan S. Conditional disruption of the prolyl hydroxylase domain-containing protein 2 (Phd2) gene defines its key role in skeletal development. *J Bone Miner Res* 2014; **29**: 2276-2286 [PMID: 24753072 DOI: 10.1002/jbmr.2258]

24 **Lee SY**, Park KH, Yu HG, Kook E, Song WH, Lee G, Koh JT, Shin HI, Choi JY, Huh YH, Ryu JH. Controlling hypoxia-inducible factor-2α is critical for maintaining bone homeostasis in mice. *Bone Res* 2019; **7**: 14 [PMID: 31098335 DOI: 10.1038/s41413-019-0054-y]

25 **Merceron C**, Ranganathan K, Wang E, Tata Z, Makkapati S, Khan MP, Mangiavini L, Yao AQ, Castellini L, Levi B, Giaccia AJ, Schipani E. Hypoxia-inducible factor 2α is a negative regulator of osteoblastogenesis and bone mass accrual. *Bone Res* 2019; **7**: 7 [PMID: 30792937 DOI: 10.1038/s41413-019-0045-z]

26 **Guo W**, Hoque J, Garcia Garcia CJ, Spiller KV, Leinroth AP, Puviindran V, Potnis CK, Gunn KA, Newman H, Ishikawa K, Fujimoto TN, Neill DW, Delahoussaye AM, Williams NT, Kirsch DG, Hilton MJ, Varghese S, Taniguchi CM, Wu C. Radiation-induced bone loss in mice is ameliorated by inhibition of HIF-2α in skeletal progenitor cells. *Sci Transl Med* 2023; **15**: eabo5217 [PMID: 38019933 DOI: 10.1126/scitranslmed.abo5217]

27 **Wu C**, Rankin EB, Castellini L, Alcudia JF, LaGory EL, Andersen R, Rhodes SD, Wilson TL, Mohammad KS, Castillo AB, Guise TA, Schipani E, Giaccia AJ. Oxygen-sensing PHDs regulate bone homeostasis through the modulation of osteoprotegerin. *Genes Dev* 2015; **29**: 817-831 [PMID: 25846796 DOI: 10.1101/gad.255000.114]

28 **Wang Y**, Wan C, Deng L, Liu X, Cao X, Gilbert SR, Bouxsein ML, Faugere MC, Guldberg RE, Gerstenfeld LC, Haase VH, Johnson RS, Schipani E, Clemens TL. The hypoxia-inducible factor alpha pathway couples angiogenesis to osteogenesis during skeletal development. *J Clin Invest* 2007; **117**: 1616-1626 [PMID: 17549257 DOI: 10.1172/jci31581]

29 **Rankin EB**, Wu C, Khatri R, Wilson TL, Andersen R, Araldi E, Rankin AL, Yuan J, Kuo CJ, Schipani E, Giaccia AJ. The HIF signaling pathway in osteoblasts directly modulates erythropoiesis through the production of EPO. *Cell* 2012; **149**: 63-74 [PMID: 22464323 DOI: 10.1016/j.cell.2012.01.051]

30 **Shen G**, Ren H, Qiu T, Zhang Z, Zhao W, Yu X, Huang J, Tang J, Liang D, Yao Z, Yang Z, Jiang X. Mammalian target of rapamycin as a therapeutic target in osteoporosis. *J Cell Physiol* 2018; **233**: 3929-3944 [PMID: 28834576 DOI: 10.1002/jcp.26161]

31 **Darcy A**, Meltzer M, Miller J, Lee S, Chappell S, Ver Donck K, Montano M. A novel library screen identifies immunosuppressors that promote osteoblast differentiation. *Bone* 2012; **50**: 1294-1303 [PMID: 22421346 DOI: 10.1016/j.bone.2012.03.001]

32 **Lee KW**, Yook JY, Son MY, Kim MJ, Koo DB, Han YM, Cho YS. Rapamycin promotes the osteoblastic differentiation of human embryonic stem cells by blocking the mTOR pathway and stimulating the BMP/Smad pathway. *Stem Cells Dev* 2010; **19**: 557-568 [PMID: 19642865 DOI: 10.1089/scd.2009.0147]

33 **Chen C**, Akiyama K, Wang D, Xu X, Li B, Moshaverinia A, Brombacher F, Sun L, Shi S. mTOR inhibition rescues osteopenia in mice with systemic sclerosis. *J Exp Med* 2015; **212**: 73-91 [PMID: 25534817 DOI: 10.1084/jem.20140643]

34 **Ivan M**, Kondo K, Yang H, Kim W, Valiando J, Ohh M, Salic A, Asara JM, Lane WS, Kaelin WG Jr. HIFalpha targeted for VHL-mediated destruction by proline hydroxylation: implications for O2 sensing. *Science* 2001; **292**: 464-468 [PMID: 11292862 DOI: 10.1126/science.1059817]

35 **Beuck S**, Schänzer W, Thevis M. Hypoxia-inducible factor stabilizers and other small-molecule erythropoiesis-stimulating agents in current and preventive doping analysis. *Drug Test Anal* 2012; **4**: 830-845 [PMID: 22362605 DOI: 10.1002/dta.390]

36 **Chen N**, Hao C, Liu BC, Lin H, Wang C, Xing C, Liang X, Jiang G, Liu Z, Li X, Zuo L, Luo L, Wang J, Zhao MH, Cai GY, Hao L, Leong R, Liu C, Neff T, Szczech L, Yu KP. Roxadustat Treatment for Anemia in Patients Undergoing Long-Term Dialysis. *N Engl J Med* 2019; **381**: 1011-1022 [PMID: 31340116 DOI: 10.1056/NEJMoa1901713]

37 **Chen N**, Hao C, Peng X, Lin H, Yin A, Hao L, Tao Y, Liang X, Liu Z, Xing C, Chen J, Luo L, Zuo L, Liao Y, Liu BC, Leong R, Wang C, Liu C, Neff T, Szczech L, Yu KP. Roxadustat for Anemia in Patients with Kidney Disease Not Receiving Dialysis. *N Engl J Med* 2019; **381**: 1001-1010 [PMID: 31340089 DOI: 10.1056/NEJMoa1813599]

38 **Provenzano R**, Besarab A, Sun CH, Diamond SA, Durham JH, Cangiano JL, Aiello JR, Novak JE, Lee T, Leong R, Roberts BK, Saikali KG, Hemmerich S, Szczech LA, Yu KP, Neff TB. Oral Hypoxia-Inducible Factor Prolyl Hydroxylase Inhibitor Roxadustat (FG-4592) for the Treatment of Anemia in Patients with CKD. *Clin J Am Soc Nephrol* 2016; **11**: 982-991 [PMID: 27094610 DOI: 10.2215/CJN.06890615]

39 **Zhang X**, Zhang Y, Wang P, Zhang SY, Dong Y, Zeng G, Yan Y, Sun L, Wu Q, Liu H, Liu B, Kong W, Wang X, Jiang C. Adipocyte Hypoxia-Inducible Factor 2α Suppresses Atherosclerosis by Promoting Adipose Ceramide Catabolism. *Cell Metab* 2019; **30**: 937-951.e5 [PMID: 31668872 DOI: 10.1016/j.cmet.2019.09.016]

40 **Su K**, Li Z, Yu Y, Zhang X. The prolyl hydroxylase inhibitor roxadustat: Paradigm in drug discovery and prospects for clinical application

beyond anemia. *Drug Discov Today* 2020; **25**: 1262-1269 [PMID: 32380083 DOI: 10.1016/j.drudis.2020.04.017]

41 **Chen C**, Yan S, Qiu S, Geng Z, Wang Z. HIF/Ca(2+)/NO/ROS is critical in roxadustat treating bone fracture by stimulating the proliferation and migration of BMSCs. *Life Sci* 2021; **264**: 118684 [PMID: 33129877 DOI: 10.1016/j.lfs.2020.118684]

42 **Hulley PA**, Papadimitriou-Olivgeri I, Knowles HJ. Osteoblast-Osteoclast Coculture Amplifies Inhibitory Effects of FG-4592 on Human Osteoclastogenesis and Reduces Bone Resorption. *JBMR Plus* 2020; **4**: e10370 [PMID: 32666021 DOI: 10.1002/jbm4.10370]

Published by **Baishideng Publishing Group Inc**
7041 Koll Center Parkway, Suite 160, Pleasanton, CA 94566, USA
Telephone: +1-925-3991568
E-mail: office@baishideng.com
Help Desk: https://www.f6publishing.com/helpdesk
https://www.wjgnet.com